

Robotic Vehicle Control using Brain Computer Interface

Rakesh Bute



Department of Electronics and Instrumentation
National Institute of Technology Rourkela

Robotic Vehicle Control using Brain Computer Interface

Thesis submitted in partial fulfillment

of the requirements of the degree of

Master of Technology

in

Electronics and Instrumentation

(Specialization: Electronics and Instrumentation)

by

Rakesh Bute

(Roll Number: 214EC3011)

under the supervision of

Dr. Samit Ari



May, 2016

Department of Electronics and Instrumentation
National Institute of Technology Rourkela



Department of Electronics and Instrumentation
National Institute of Technology Rourkela

Dr. Samit Ari

May 26, 2016

Supervisor's Certificate

This is to certify that the work presented in the dissertation entitled *Robotic Vehicle Control using Brain Computer Interface* submitted by *Rakesh Bute*, Roll Number 214EC3011, is a record of original research carried out by him under my supervision and guidance in partial fulfillment of the requirements of the degree of *Master of Technology in Electronics and Instrumentation*. Neither this thesis nor any part of it has been submitted earlier for any degree or diploma to any institute or university in India or abroad.

Samit Ari

Declaration of Originality

I, *Rakesh Bute*, Roll Number *214EC3011* hereby declare that this dissertation entitled *Robotic Vehicle Control using Brain Computer Interface* presents my original work carried out as a postgraduate student of NIT Rourkela and, to the best of my knowledge, contains no material previously published or written by another person, nor any material presented by me for the award of any degree or diploma of NIT Rourkela or any other institution. Any contribution made to this research by others, with whom I have worked at NIT Rourkela or elsewhere, is explicitly acknowledged in the dissertation. Works of other authors cited in this dissertation have been duly acknowledged under the sections “Reference” or “Bibliography”. I have also submitted my original research records to the scrutiny committee for evaluation of my dissertation.

I am fully aware that in case of any non-compliance detected in future, the Senate of NIT Rourkela may withdraw the degree awarded to me on the basis of the present dissertation.

May 26, 2016
NIT Rourkela

Rakesh Bute

Acknowledgment

I would first like to thank my thesis advisor Dr. Samit Ari of Signal and Image Processing. The door to Dr. Ari office was always open whenever I ran into a trouble spot or had a question about my research or writing. He consistently allowed this paper to be my own work, but steered me in the right the direction whenever he thought I needed it.

I would also like to thank the experts who were involved in the validation experiments for this research project Sourav Kundu (PhD Student). I would like to thank Neha Gupta (PhD Student) and Dipak Kumar Ghosh (PhD Student) for their support for extended work hours. I would also like to thank my friend Sudhansu Mallik, Ujjwal Kumar Durgam and Amrit Chakraborty for helping me by being subjects of experiment.

I would like to express my gratitude and respect to Prof. K.K.Mahaptra, Prof. S.K.Patra, and Prof.A.K. Sahoo, Prof. L.P.Roy, Prof. S. Maiti, Prof. A.K. Swain, Prof. D.P.Acharya, Prof.T.K.Dan, Prof.U.C.Pati, for their guidance and suggestions throughout the M.Tech course. I would also like thank all the faculty members of the EC department, NIT Rourkela for their support during the tenure spent here.

Finally, I must express my very profound gratitude to my parents for providing me with unfailing support and continuous encouragement throughout my years of study and through the process of researching and writing this thesis. This accomplishment would not have been possible without them. Thank you.

May 26, 2016
NIT Rourkela

Rakesh Bute
Roll Number: 214EC3011

Abstract

Brain Computer Interface (BCI) is an interfacing device that interacts with external device or computer. The principle of Brain Computer interface is based on Electroencephalography. Under the influence of external stimuli, human brain generates some responses on distinctive areas of the brain. These responses appear in the EEG signals captured from corresponding electrode positions on the scalp of the human subject. The responses appear in the EEG signal as a feature in the time domain, or a feature in the frequency domain depending upon the periodic nature of the stimuli. These features are then detected classified and then control signal is generated by an external device. This enables the subject to directly control an external device from the brain using the signals generated in response to stimulation.

Brain-computer Interface has shown promising application to aid patients with Locked-in syndrome, Spinal Cord Injury (SCI), Acute Inflammatory Demyelinating Polyradiculoneuropathy (AIDP), Lock-down Syndrome and Amyotrophic Lateral Sclerosis (ALS). Until now, these patients needed human assistance to communicate. Brain-computer interface also has promising application for wheelchair control. Where these patients would be able to control electric wheelchairs using Brain Computer interface. In this work, a working model of Brain Computer Interface has been developed using PowerLab 16/35 and ML-138 bio-amplifier. The BCI is based on Steady State Visually Evoked Potential (SSVEP). SSVEP response is generated from the visual cortex of the subject when the subject is exposed to a flickering light source. A model robotic platform has also been controlled using the detected SSVEP Signal.

Keywords: SSVEP; Brain Computer Interface; Robotic Vehicle Control.

Contents

Supervisor's Certificate	ii
Declaration of Originality	iii
Acknowledgment	iv
Abstract	v
List of Figures	ix
List of Tables	xi
1 Introduction	1
1.1 Brain Computer Interface	1
1.2 Visually Evoked Potential	2
1.2.1 P300	2
1.2.2 SSVEP	3
1.3 Objective	4
1.4 Literature Survey	4
2 Data Acquisition	6
2.1 User Interface	6
2.1.1 Visual Component	6
2.1.2 Matlab Integration with User Interface	8
2.1.3 Hardware Inetrfacng for Data Acquisition	9
2.2 Skin Preperation and Electrode Placement	9

2.2.1	Electrolyte Selection	11
2.2.2	Skin preperation	11
2.2.3	Electrode Selection	12
2.2.4	Electrode Positioning and Placement	13
2.3	Hardware	16
2.4	Software and Storage	19
2.5	Acquired Data	19
3	Robotic Vehicle Control	25
3.1	Robotic Vehicle	25
3.1.1	Power Requirements	26
3.2	Speed Control	29
3.3	Operation	29
3.4	Methodology	32
3.4.1	Preprocessing	34
3.4.2	Mathematical Model	34
3.5	Results	36
3.5.1	Standard Database	37
3.5.2	Developped Database	37
3.6	Discussion	38
4	Conclusion and Future Work	45
4.1	Conclusion	45
4.2	Future work	45
	References	47

Abbreviations

BCI	Brain Computer Interface
SSVEP	Steady State Visually Evoked Potential
TTL	Transistor Transistor Logic
EEG	Electroencephalogram
ICA	Independent Component Analysis
PCA	Principal Component Analysis
DAQ	Data Acquisition System
MCTW	Multi Class T-Weight
UI	User Interface
UART	Universal Asynchronous Receiver and Transmitter
SNR	Signal To Noise Ratio
EM	Electromagnetic
VEP	Visually Evoked Potentials
AIDP	Acute Inflammatory Demyelinating Polyradiculoneuropathy
SCI	Spinal Cord Injury
ALS	Amyotrophic Lateral Sclerosis

List of Figures

1.1	Typical waveform of visually evoked potential.	2
2.1	Aesthetic view of the User Interface.	8
2.2	Flow chart of User Interface Operations	10
2.3	Standard 10-20 BCI Cap	12
2.4	Cup Electrode	13
2.5	Electrode Positions for data acquisition. The positioning follows 10-20 Electrode Cap Standard.	15
2.6	Picture of the PowerLab 16/35 Data Aquisition System (top) and the Octal Bio Amplifier ML-138	16
2.7	Live experiment.	17
2.8	Graphical View of Experimental Setup	18
2.9	Recorded EEG waveform of Oz Electrode for 6 Hz SSVEP stimulation	20
2.10	Recorded EEG spectrum of Oz Electrode for 6 Hz SSVEP stimulation .	20
2.11	Recorded EEG waveform of Oz Electrode for 6.5 Hz SSVEP stimulation	21
2.12	Recorded EEG spectrum of Oz Electrode for 6.5 Hz SSVEP stimulation	21
2.13	Recorded EEG waveform of Oz Electrode for 7 Hz SSVEP stimulation	22
2.14	Recorded EEG spectrum of Oz Electrode for 7 Hz SSVEP stimulation .	22
2.15	Recorded EEG waveform of Oz Electrode for 7.5 Hz SSVEP stimulation	23
2.16	Recorded EEG spectrum of Oz Electrode for 7.5 Hz SSVEP stimulation	23
2.17	Recorded EEG waveform of Oz Electrode for 8.2 Hz SSVEP stimulation	24
2.18	Recorded EEG spectrum of Oz Electrode for 8.2 Hz SSVEP stimulation	24
3.1	Robotic Vehicle	26

3.2	Controler (Arduino Pro Mini)	27
3.3	USB to TTL converter module	28
3.4	Motor Driver Unit	28
3.5	Picture of DC-DC Step Down Switching Voltage Regulator	30
3.6	Reference Circuit Diagram of DC-DC Step Down Switching Voltage Regulator	30
3.7	Circuit Diagram of Robotic Unit	31
3.8	Control Flow Diagram	33
3.9	EEG Spectrum of Oz Channel for 6 Hz Excitation Source	39
3.10	Classifier Scores for Each Class with dominant 6 Hz Class	40
3.11	EEG Spectrum of Oz Channel for 6.5 Hz Excitation Source	40
3.12	Classifier Scores for Each Class with dominant 6.5 Hz Class	41
3.13	EEG Spectrum of Oz Channel for 7 Hz Excitation Source	41
3.14	Classifier Scores for Each Class with dominant 7 Hz Class	42
3.15	EEG Spectrum of Oz Channel for 7.5 Hz Excitation Source	42
3.16	Classifier Scores for Each Class with dominant 7.5 Hz Class	43
3.17	EEG Spectrum of Oz Channel for 8.2 Hz Excitation Source	43
3.18	Classifier Scores for Each Class with dominant 8.2 Hz Class	44

List of Tables

2.1	Electrodes used in single channel SSVEP Detection and their position on the scalp	14
2.2	Data Acquisition Settings	17
3.1	Details of participants in the multitarget standard database	37
3.2	Correct Detection Per User using Author's [1] method on standard database	37
3.3	Correct Detection Per User using modified method on standard database	38
3.4	Details of participants in the multitarget standard database	38
3.5	Correct Detection Per User using modified method on generated database	38

Chapter 1

Introduction

People with spine injuries many times suffer 'Lock-down Syndrome' where their limbs get partially or fully paralysed. This restricts them leaving their bed and wheelchair. Added to this, communicating with other people becomes difficult for them because many times, they partially or completely lose the ability to speak as well. But they are still able to hear or see. There are other medical conditions can also create such symptoms as the Lock Down Syndrome[1].

These disease or medical conditions restricts the patient to leave their bed or wheelchair. Added to that, these patients are dependent upon human assistance for even communicating with other persons as well. To communicate, the helping person stands with a board with all the letters numbers and few other options inscribed in the board. Then he or she points out different options and the patient blinks to indicate whether he selects or rejects the option currently pointed. It takes minutes to spell a single word. The patients are dependent on others for their movement as well. They are bed ridden for their life. Mobility itself is a problem for them.

1.1 Brain Computer Interface

To provide assistance to the patients with 'Lock-down Syndrom', scientists are trying to develop Brain Computer Interface system that can eliminate the need of human assistance to figure out the choice the patient wants to select. Brain Computer Interfaces target to provide an alternative input device, which will not rely upon

mechanical movements for input [2].

1.2 Visually Evoked Potential

The brain-computer interface signals rely upon Visually Evoked Potentials (VEP), thus, if the patient can move their eyeball, they can use the system. The concept is that the patient would be given the options on a board, arranged in the grid, with bright light flashing in the area around them. The patient then would look at the option he wants to choose. The flashing light would then help generate a visually evoked potential in his visual cortex[3, 4]. There are two types of visually evoked potential obtained, P300 and SSVEP (Steady-State Visually Evoked Potential)[5].

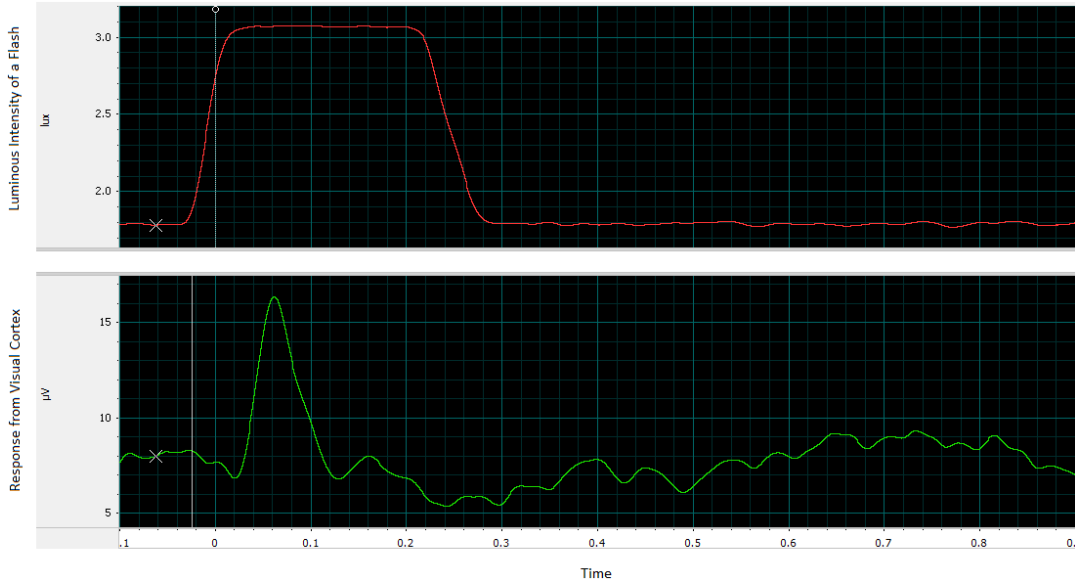


Figure 1.1: Typical waveform of visually evoked potential.

1.2.1 P300

P300 is a feature in the Electro Encephalogram Signal acquired from the visual cortex[6, 7]. It appears as a peak in the signal after a flash has been seen by the patient. The time difference between the flash and the signal appearing is approximately 300mS. Intercepting P300 signal requires that the p300 stimulations are time stamping

by the user interface. The complexity of intercepting P300 signal is more compared to other visually evoked potentials.

1.2.2 SSVEP

SSVEP is evoked from the visual cortex of the human brain in resonance to the stroboscopic visual stimulation. When a person pays his attention to a periodic flashing light with a frequency of 4-60 Hz, the recorded Electroencephalogram signal of that person would show that a periodic component is appearing in the visual cortex region of the Electroencephalogram signal [8–10]. The frequency of the component would be same as the flickering frequency of the flashing light. If we calculate the Fourier Transform of the acquired EEG signal and observe the spectrum, we could also find peaks at the harmonic frequencies of the flickering frequency.

SSVEP signals are most robust among other types of visually evoked potentials. It is likely to be detected correctly despite variations in amplitudes, and jitter in frequency response. It has been observed it can tolerate low Signal to Noise ratio up to some extent.

SSVEP signals appear in the spectrum of the eeg signal as multiple peaks in them. As EEG is invoked in resonance to the flickering frequency, the peaks that appear in the ssvep signal has mathematical relation. The location of the peaks are integer multiples of the stimuli of the fundamental frequency, which is equal to the flickering frequency of the source signal.

To process the ssvep signal, typical classification procedure is followed. Static SSVEP signal detection is basically a one-dimensional, frequency domain feature extraction followed by class construction and then classification. To classify an SSVEP signal for multitarget detection, multiple classes are constructed from selected feature points. For each class, the feature is selected by narrow windows selecting small bands around the fundamental frequency and it's harmonics. The windows that lies on the harmonic frequencies of a fundamental frequency, is included in the class to detect the corresponding harmonic frequency.

The response of the SSVEP is strongest at the visual cortex. In standard 10-20 EEG cap, the corresponding electrode position is Oz. To receive a strong signal, it is important to identify the position and place the electrodes properly. SSVEP Detection could use single or multichannel EEG detection. There are multichannel EEG measurements proved to be more accurate than single channel. Multichannel measurements provide sufficient data to cancel EEG artifacts and nuisance signals. But for classification, only the preprocessed Oz signal is used.

The SSVEP response to a range of flickering frequency varies from person to person. Also, the SSVEP response is seen to be most prevalent in 5.6-15.3Hz with a peak response for 12 Hz, and with weakest responses at 28Hz and 42Hz[8].

1.3 Objective

The expected end result of this work is to provide a Brain Computer Interface, an alternative way to interact with the computer. The system would be used by the patients with Lock Down Syndrome without any electronics implant. Brain Computer Interface can acquire signal without any implants in the human body. Also, it can operate without any physical movement. The expected end result of this research is to provide them with an electric wheel chair, that they can operate even after losing control over all of their limbs and their body, without any surgical implants.

1.4 Literature Survey

Brain Computer Interface has been studied since JJ Vidal [11] has studied possibilities to use EEG signal in controlling computers in his paper "Toward direct brain-computer communication". The Visually Evoked Potential has been first described in his paper [11].

Though, detailed study has not been performed on SSVEP by anyone before Christoph S Herrmann [12]. He first characterised the SSVEP response for 1-100 Hz flickering frequency. His study has first shown that the SSVEP response contains

the fundamental frequency and the harmonics. From his paper, it has been observed that the harmonics contain a significant amount of energy in them. Also, the response has been strong in 5 to 60 Hz band. Also, the second harmonics has been seen to be strong up to 75 Hz.

The next major progress in the SSVEP based Brain Computer Interface has been done by Ola Friman et.al [13]. For the first time, a visually evoked potential has been mathematically modelled. His model has included fundamental frequency and it's harmonics into the calculation. Alongside noise, he also modelled the interfering signal from the other part of the brain to the visually evoked potential in his paper. A mathematical model has also been suggested to cancel out the nuisance signal. To cancel out nuisance signal, his study made use of multi-channel SSVEP.

Another qualitative study on SSVEP is done by Hovagim Bakardjian, Toshihisa Tanakaa and Andrzej Cichockia. In their study [8], they have shown that the SSVEP response is not uniform throughout the frequency range, rather, it peaks in 12 Hz and diminishes at 28 and 42 Hz. The optimal band for SSVEP excitation source have found to be 5.6-15.3 Hz.

For practical purpose, the eeg signal needs to be preprocessed, and noise must be filtered out for further processing. For noise removal, various algorithms have been developed for processing frequency domain and time domain EEG signal. Recently, statistical signal processing has also been adopted for noise removal. Usage of Independent Component Analysis (ICA) and Principal Component Analysis (PCA) has been proposed for ocular artifact removal and ECG artifact Removal [14–16]. ICA and PCA techniques are blind source separation techniques. There are other blind source separation techniques are present that can be used with the eeg signal ,for artifact removal [17, 18]. Apart from blind source separation, Parallel Factor Analysis has also been popular for EEG artifact removal [17]. Wavelet Transform combined with Independent component analysis [19] and Wavelet Transform [20] has also been used for EEG artifact Removal. Apart from non adaptive eeg artifact removal, adaptive artifact removal is also used [21].

Chapter 2

Data Acquisition

The data acquisition for SSVEP based brain computer interface requires an user interface, a data acquisition system and a computer. The user interface shall be able to produce SSVEP stimulations required for data acquisition, the hardware used are PowerLab 16/35, ML 138 Octal Bio Amplifier and Standard 10-20 EEG Cap [22] [23].

2.1 User Interface

The user Interface is designed using java swing. It has capabilities to invoke Matlab and labchart interface automatically at startup. It integrates the whole process of generating stimuli, data acquisition and analysis using already available application programs. The user interface uses Matlab control library and java json library to implement its functionality.

2.1.1 Visual Component

While loading, the User Interface loads settings from ‘settings’ folder, if no settings file is supplied with ‘-settings’ switch, the User Interface assumes ‘settings default.json’ as default settings file. Currently, the user interface looks for four sections.

- **‘uioptions’** This section controls the general functionality of the program. It controls the following operations.

- ‘horizontalgap’ The width of the horizontal gaps between the flickering areas of each option.
 - ‘verticalgap’ The height of the vertical gaps between the flickering areas of each option.
 - ‘detectionrecess’ This option determines the interval between two adjacent sessions of flickering
 - ‘Matlabscript’ The name of the Matlab script inside ‘script’ folder, which would be called at session startup, data acquisition events and at session end.
- **‘singletonmodel’** This section describes the structure of each option to the User interface. It consists of the following major components.
 - ‘symbol’ The symbol the option would be flickering. It is useful for testing purposes. The symbol is programmatically replaced later.
 - ‘elements’ The element option points to an array that holds the definition of other visual elements. The visual elements are layered in order they are defined, the first component at the top. Each visual elements have their specific properties declared in their definition.
 - **‘keys’** This section describes what symbols are to be presented by the user interfaces and their position. They are arranged in form of two dimensional array. It is possible to use UTF-16 symbol. This increases the scope for using multilingual symbols and signs.
 - **‘groupmodel’** The group model holds the details of the flashing groups. Each group has name and the group structure is described by the following fields.
 - ‘SignalType’ The type of excitation the group is supposed to provide. It could be either SSVEP or P300.
 - ‘flashingLayer’ The layer of the singletons used by the group to flash.

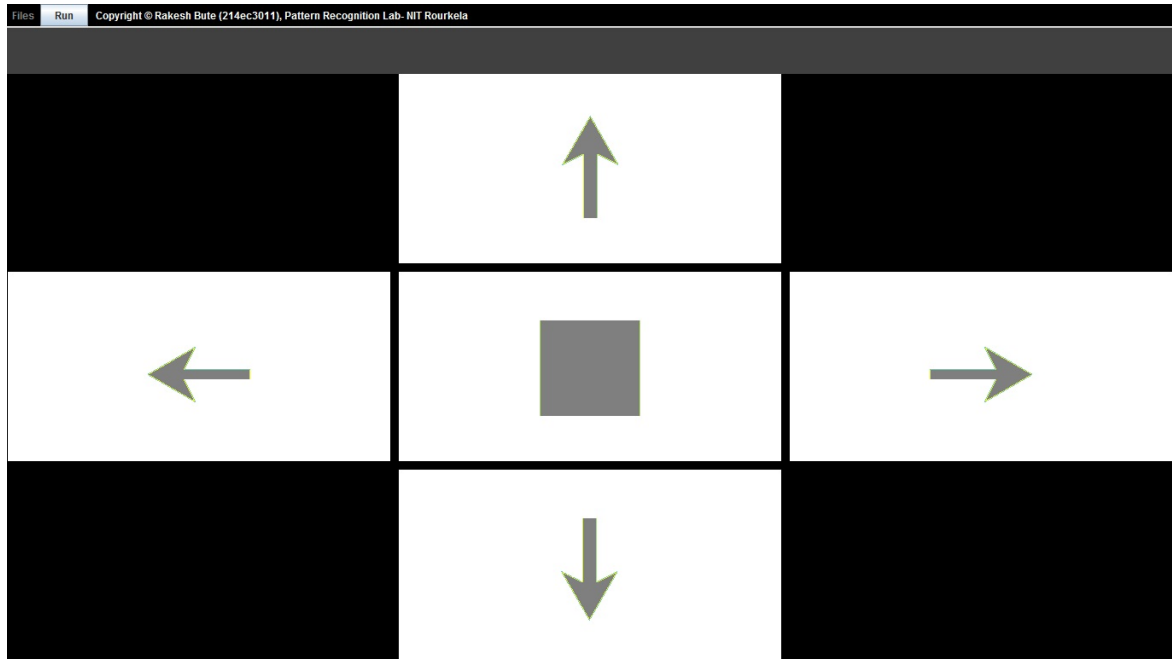


Figure 2.1: Aesthetic view of the User Interface.

- ‘frequencies’ This section determines the frequency of flicker. For SSVEP stimulation, different values are permitted. For P300 stimulation, all the frequency values are kept same. A frequency below 4 Hz causes the group to stop flicker.
- ‘members’ This section is supported so that in future, the same UI could be used for more complex experiments and application. This section is a three dimensional array. Each array of first dimension holds the list of indexes (i.e. positions of singletons) that are member of the sub flickering groups. This type of grouping would allow future complex application of this user interface such as BCI Speller application.

2.1.2 Matlab Integration with User Interface

The user interface uses ‘Matlabcontrol’ library for invoking Matlab session. On successful invocation Matlab, a Matlab session object is created and returned by ‘MatlabProxyFactory’. Basically, the Matlab proxy object helps to call two functions in the Matlab session. one is ‘eval’ and another is ‘feval’. The ‘eval’ function supports

both Matlab function and Matlab script calling and Matlab function calls. While the 'feval' only calls Matlab functions. When we need an output, the 'feval' must be called. For this experiment, no output is expected, and the Matlab scripts are called using 'eval' function call.

When Matlab session is starting, the Matlab directory is changed to the 'scripts' directory. All the necessary Matlab scripts need to be run by Matlab must be present in that directory. The user interface looks into the settings file for a pilot script which can run the experiment. The pilot script is called when starting a data acquisition session, ending a data acquisition session, and after each run of flashing.

2.1.3 Hardware Inetrfacing for Data Acquisition

The hardware used in this experiment uses PowerLab 16/35 as a DataAcquisition device. The device does not provide any java api for interfacing, but it is possible to acquire data using com objects generated by 'activex' server. And Matlab has inbuilt support for creating com objects, accessing it's fields, and register function handles. To acqurie data using Matlab, first a com object of type 'ADICChart.Document' needs to be created. it is done using 'actxserver' function call. The 'actxserver' then starts a LabChart Session, opens a LabChart ocument with default settings and returns the object to the Matlab.

After the 'activex' object has been created, three functions are registered for being called when data acquisition session starts, data acquisition session stops, and at data arives in short bursts. The data is supplied to the Matlab functions in form of key value pairs. So the data must be accessed using inbuilt Matlab varargin command.

2.2 Skin Preperation and Electrode Placement

In electroencephalogram, skin preparation and proper electrode placement assures good selectivity of EEG signal and good sugnal quality. There are some factors needs to be kept in mind while choosing materials and equipment for a good signal acquisition.

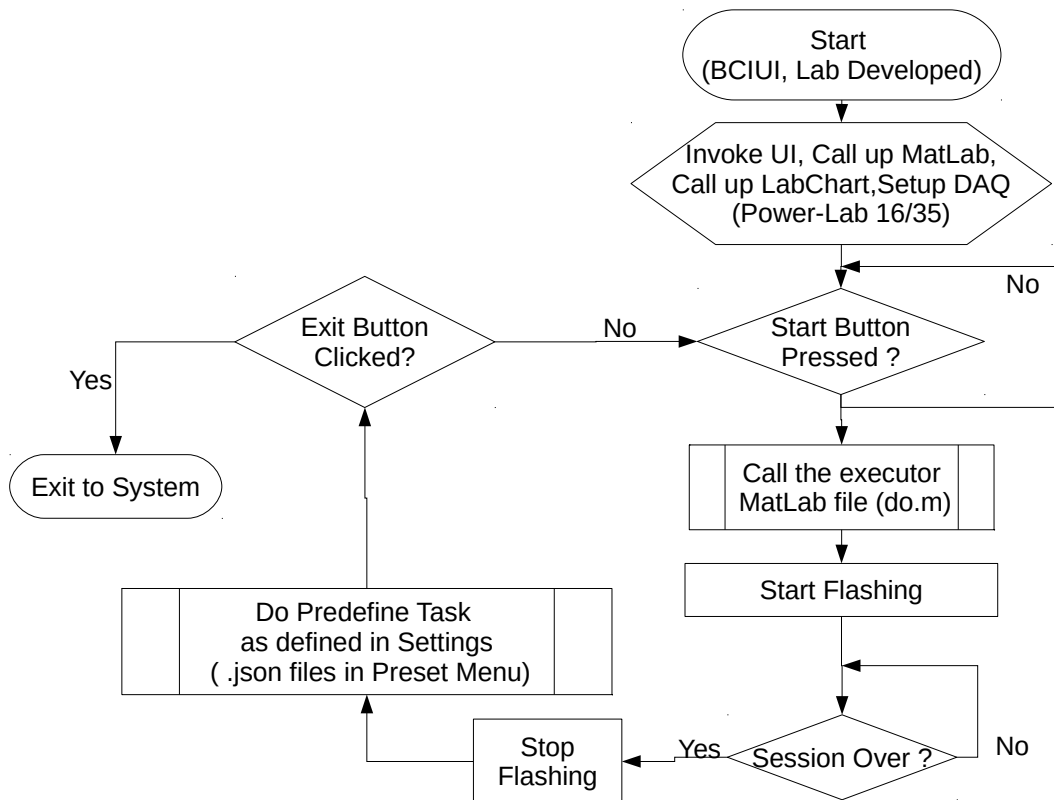


Figure 2.2: Flow chart of User Interface Operations

2.2.1 Electrolyte Selection

In electrolyte, the electricity conduction is done by ions. Thus, less viscosity results in less resistance and better electrodes. It is not possible to use a liquid as it would spill out of electrode and might make an electrical path to other electrode location. The viscosity is chosen depending upon the need of the data acquisition. The salt in the electrolyte is mostly Silver Chloride as it is non-toxic for body fluid. However, depending upon viscosity, there are two types of electrolyte.

- *Electrode gel* It provide better conductivity and can achive electrode impedance as low as $2.5\text{ K}\Omega$. However, too much of gel might spill from the electrodes and create undesired short circuit with other electodes. It could be used with BCI caps. If the gel is required to be used without BCI cap, a pice of surgical gauge is soaked with gel and applied on the electrode.
- *Electrode paste* It provide less conductivity but it does not spill. Due to more viscosity it can hold electrodes in place if they are not agitated. Cup electrodes cannot be used without electrode paste. The electrode paste, on avarage, provide a conductivity of $30\text{ K}\Omega$. If conductivity is required to increase, electrode gel is spilled over the electrode and on the adjuscent area, and it is covered with surgical gauge to stop spilling.

2.2.2 Skin preperation

Human skin is oily and it always shed tissues. Sheddigng tissues are dead cells and they eventually dry out. As a result, thease tissues make a non conducting layer on the skin that increases electrode impedance. Moreover, oil and dirt makes thease tissues stick on the skin and they themselfe are bad conductor. To make a good contact with the electrolyte, the skin is first scrubbed to remove the dirt, dead tissues and oil from the skin.



Figure 2.3: Standard 10-20 BCI Cap

2.2.3 Electrode Selection

The electrode selection is basically made based upon the need of electrode channels. If the data acquisition requires three or more electrodes, electrode cap is preferred. Otherwise, cup electrodes are used. Here are some details about the electrodes.

- Electrode cap** It is made of stretchable cloth, stitched with electrodes. In a standard 10-20 BCI electrode cap there are 19 electrodes in a cap. When recording data, one of these electrode is connected to ground terminal of the bio-amplifier, and a clip electrode is connected to either of the ears for reference voltage. The metal used in these electrodes is silver. The electrodes provide a small hollow chamber to contain the gel. The electrodes in electrode cap have a hole in the middle so that electrode gel can be put between the electrode and the skin. The lead wires connected to the electrodes form a ribbon, and its end is attached to a connector. A syringe with a blunt needle is used for filling up the gap. The rules followed in determining the electrode position is discussed in a later section.
- Cup Electrode** These electrodes are made of small bent disc to form a concave shape so that it can hold some extra electrode paste can be contained in them.



Figure 2.4: Cup Electrode

Extra electrode paste helps the electrode to stick to the skin. Cup electrodes are gold plated and have a lead wire attached to them so that they can be connected to the bio-amplifier. This type of electrode is ideal if a small number of electrodes are to be placed.

- **Clip Electrode** It can only be attached in the ear. The electrolyte is first squished into the cup of the electrode, and then it is clipped on the ear. It is only used with electrode cap.

2.2.4 Electrode Positioning and Placement

The 10-20 electrode cap is internationally recognized and a standard for electrode placement on the human scalp for EEG data acquisition. It is named so because the distance between two adjacent electrode is either 10% or 20% of the distance measured across skull from front to back or left to right. The electrodes at the right are denoted by even subscript numbers, and the electrodes in the left are denoted by odd subscript numbers. The subscript 'z' (zero) refers to the electrodes placed on the plane of symmetry in the human body.

Table 2.1: Electrodes used in single channel SSVEP Detection and their position on the scalp

Electrode Name	% Distance measured from inion
Oz	10%
Pz	30%
Cz	50%
Fz	70%
AFz	90%

Electrode Cap Placement

While using the electrode cap, the distance between nasion and inion is measured by a tape. One end of the tape is placed on the nasion, then placed through body's axis of symmetry, and then held at inion. The ribbon is then marked at the inion end and measured the distance between nasion and inion. The 10% of the distance is noted. While placing the cap on the subject's head, the electrodes at 10% ring is adjusted carefully so that they are positioned on the 10% distance measured previously.

After electrode cap is placed, the space between the electrodes and the scalp is filled using gel using a syringe and a blunt needle. Before filling up the gap, the syringe is inserted in the electrode hole and tilted to and fro to reach upto scalp. After placing electrodes, the electrode impedance of all electrodes should be checked to confirm good conductivity and proper connection.

Cup Electrode Placement

To place cup electrodes, first the position of the electrodes needs to be determined. For this, first, the nasion to inion distance is measured as shown in figure 2.7. The distances measured between them is as below.

The cup electrodes needed to be cleaned before use. The electrode positions are scrubbed with skin preparation gel to remove any oil or dirt. Then the cup electrodes are filled with electrode paste and then it is gently pressed against the skin on the electrode positions. Electrode pastes are used so that the cup electrodes doesn't creep away from their position. However, agitating the electrodes might make the electrodes

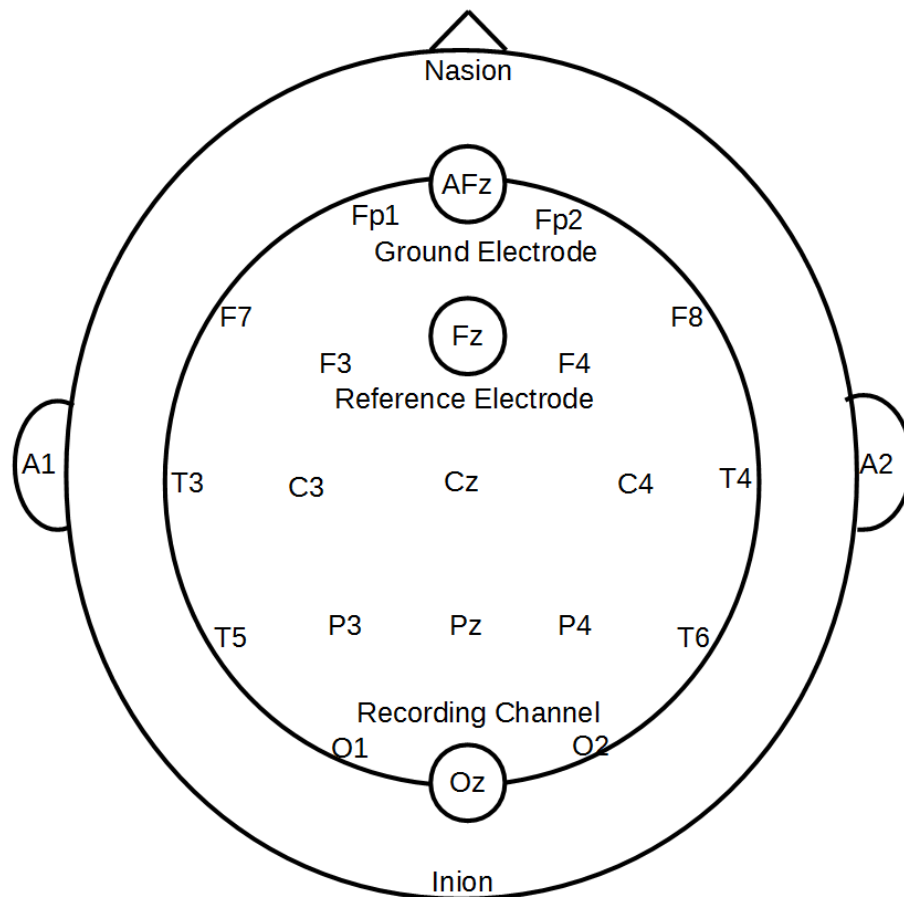


Figure 2.5: Electrode Positions for data acquisition. The positioning follows 10-20 Electrode Cap Standard.



Figure 2.6: Picture of the PowerLab 16/35 Data Acquisition System (top) and the Octal Bio Amplifier ML-138

to fall off. If only electrode paste is used, the input impedance could be much higher. To reduce the electrode impedance, a piece of surgical cloth is soaked with electrode gel and placed on the cup electrodes so that the electrode gel makes contact with the electrode and the skin surrounding it.

2.3 Hardware

The Data acquisition hardware consists of an octal bio-amplifier (ML138), and the data acquisition device PowerLab 16/35. PowerLab 16/35 is powered by AC mains, and it uses USB to connect to the computer. The PowerLab 16/35 is capable of maximum 400 Samples/S. it is capable of sampling at most 16 channels and its full-scale measurement is adjustable as high as 10V down to 2mV. The resolution of the measure could be 16 or 24 as per the settings. It is capable of sampling different channels at a different sampling frequency.

The octal Bio amplifier comes with an inbuilt amplifiers and filter. It offers electrical isolation, bio amplifier, powerline notch filtering. It's connected to the Data acquisition system by coaxial cables and an I²C connection. The bio amplifier draws required power from the Data Acquisition Device through the I²C connection.

Figure 2.7: Live experiment.



While attaching the electrodes, the impedance is kept below $5\text{ k}\Omega$ and the residual voltages are kept below 10mV . The electrode positions are AFz for ground, Fz for reference voltage Oz for the signal acquisition. The data is bandpass filtered using the internal filters of bio amplifier. The SSVEP response is strong in $4\text{-}60\text{ Hz}$. So any sampling frequency beyond 150 Hz would reliably sample it. Below are the details of parameters while sampling.

Table 2.2: Data Acquisition Settings

Parameters	Value
Sampling Frequency	400 Hz
Lower Cutoff Frequency	1 Hz
Upper Cutoff Frequency	60 Hz
Power Line Rejection	yes, 50 Hz
Electrode Impedance	$< 5\text{ K}\Omega$
Electrode Position	Oz

To invoke the SSVEP Signal, a java based User interface has been developed to present options with its surrounding area flashing at a particular frequency. The user interface is so designed that it can rearrange itself depending upon the settings file chosen. The color, flashing frequency, duration of flash, Options presented in the UI and the shape of the area behind the option can be controlled using a settings file in json format.

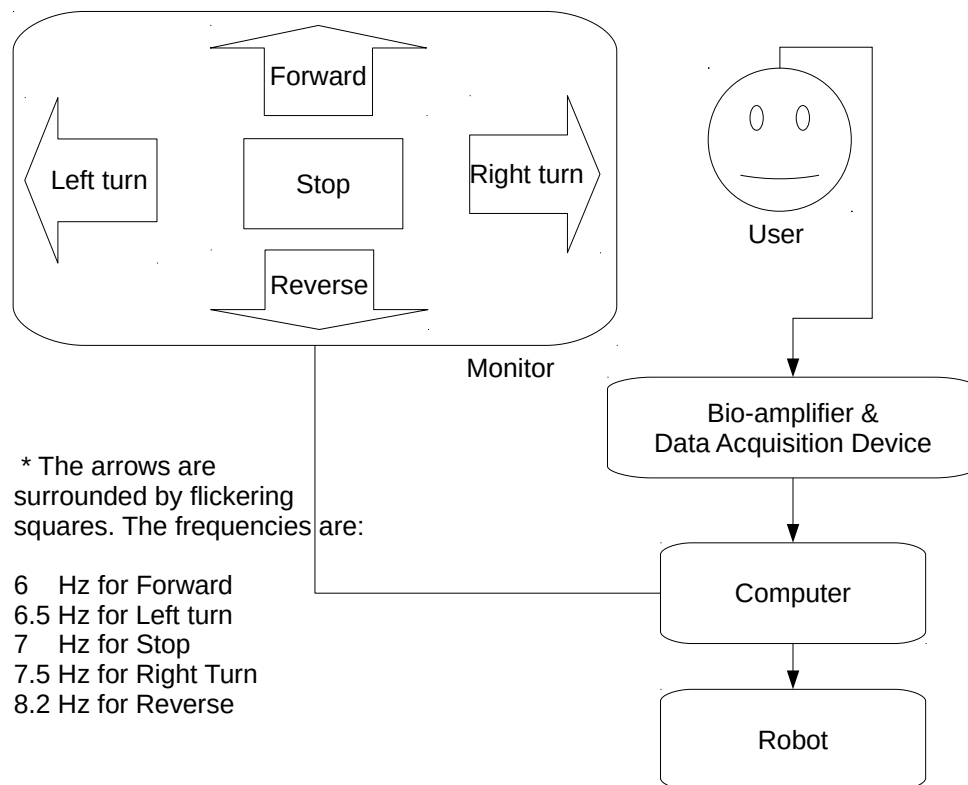


Figure 2.8: Graphical View of Experimental Setup

2.4 Software and Storage

The PowerLab 16/35 comes with its own proprietary software named LabChart. There is no direct method or api that allows Java programs or Matlab to interface the hardware directly. The software, however, through 'activex' service, allows limited control and data acquisition tasks to be performed by matlab. In case of real time analysis, Lab chart provides some basic measurement and plotting. It can perform frequency domain analysis, limited mathematical calculation, can show waveform, and save recorded session data. The procedure for data acquisition by using Matlab is already discussed in section 2.1.2. It is possible to alter the matlab scripts to perform only data acquisition instead of real time analysis.

2.5 Acquired Data

The following samples are recorded from a 25year old male subject. The eeg electrode is Oz Electrode. The Figure 2.9 shows the recorded waveform when the subject is looking at the option flickering at 6Hz. Figure 2.10 shows the corresponding spectrum calculated using Fast Fourier Transform. The data is recorded also for 6.5Hz, 7Hz, 7.5Hz and 8.2Hz SSVEP targets. The corresponding recorded waveforms are shown in Figure 2.11, Figure 2.13, Figure 2.15 and in Figure 2.17. The waveforms of these frequencies are shown in Figure 2.12, Figure 2.14, Figure 2.16 and in Figure 2.18.

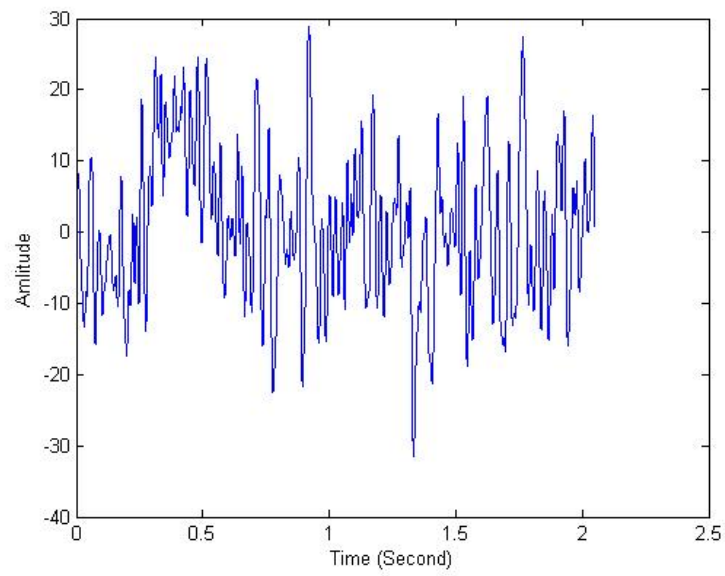


Figure 2.9: Recorded EEG waveform of Oz Electrode for 6 Hz SSVEP stimulation

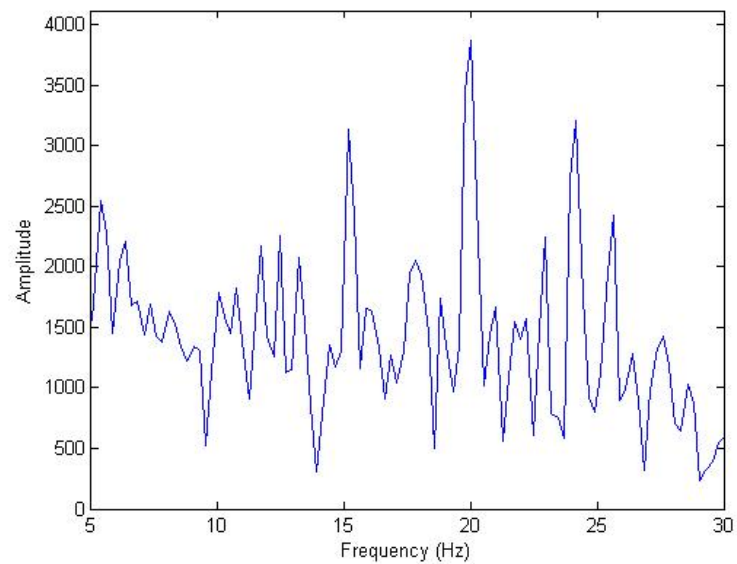


Figure 2.10: Recorded EEG spectrum of Oz Electrode for 6 Hz SSVEP stimulation

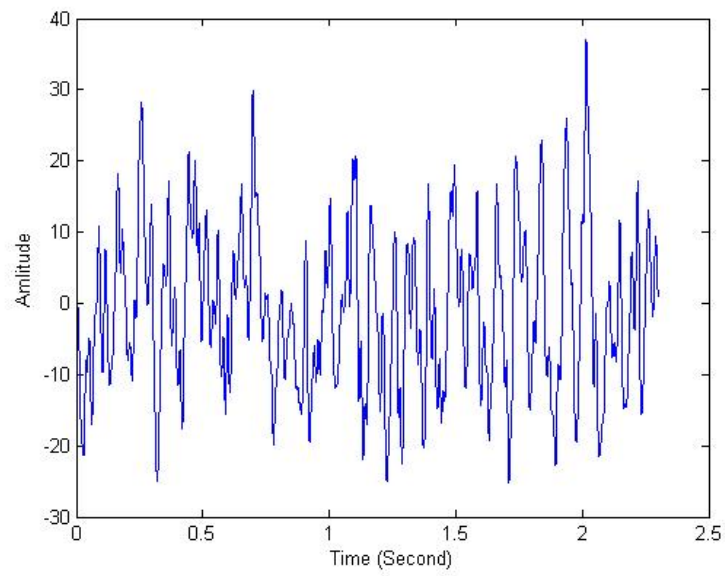


Figure 2.11: Recorded EEG waveform of Oz Electrode for 6.5 Hz SSVEP stimulation

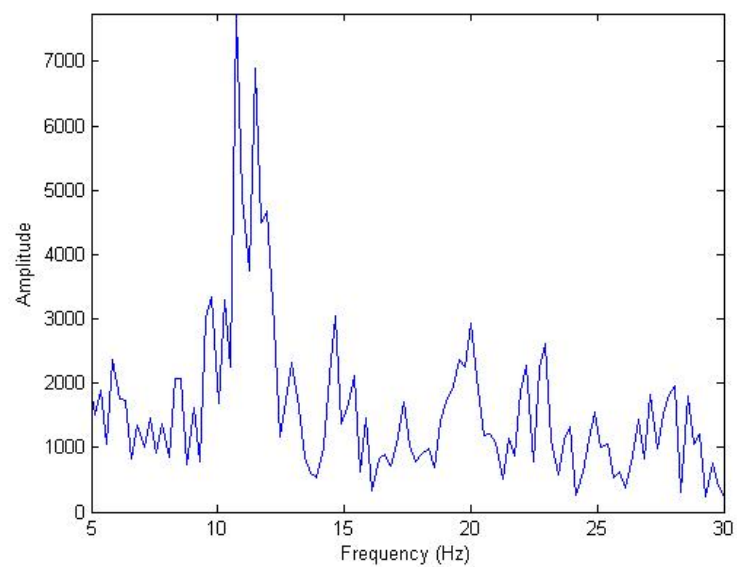


Figure 2.12: Recorded EEG spectrum of Oz Electrode for 6.5 Hz SSVEP stimulation

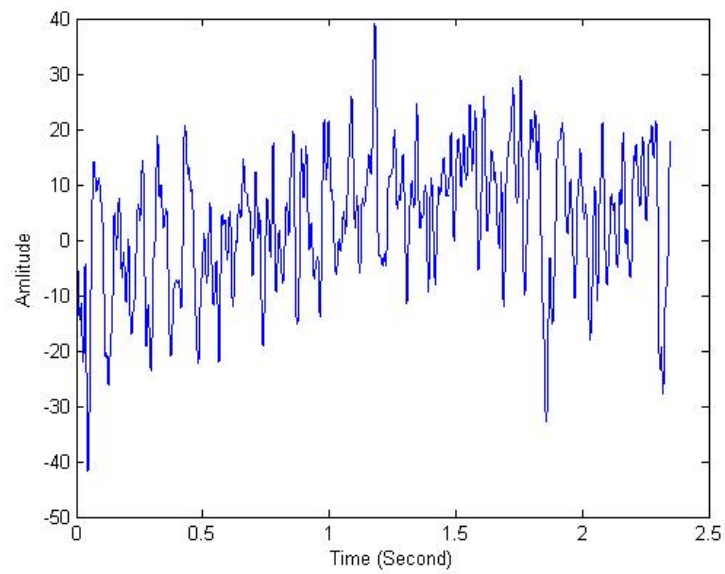


Figure 2.13: Recorded EEG waveform of Oz Electrode for 7 Hz SSVEP stimulation

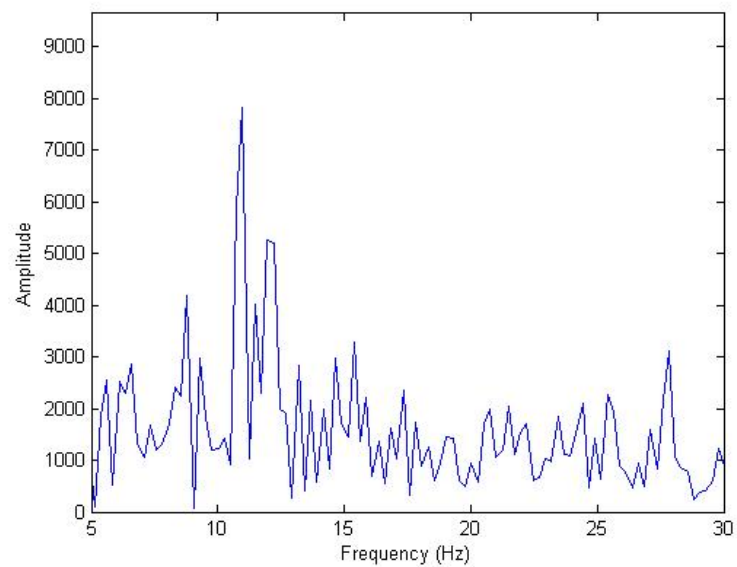


Figure 2.14: Recorded EEG spectrum of Oz Electrode for 7 Hz SSVEP stimulation

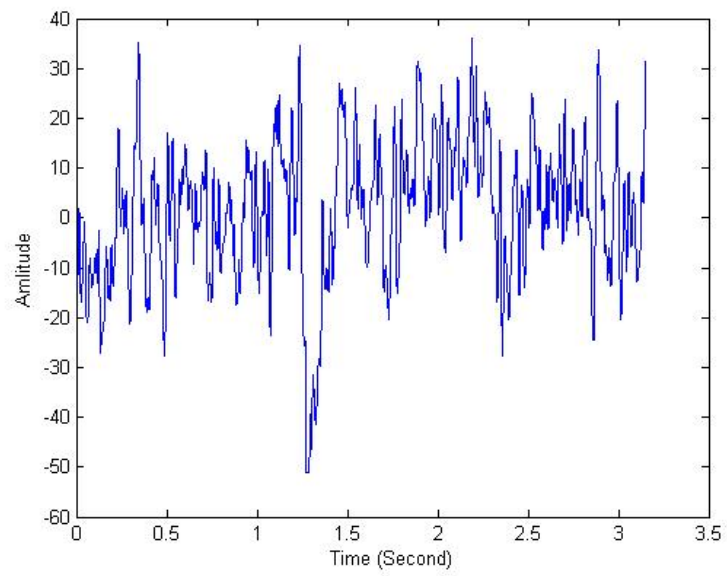


Figure 2.15: Recorded EEG waveform of Oz Electrode for 7.5 Hz SSVEP stimulation

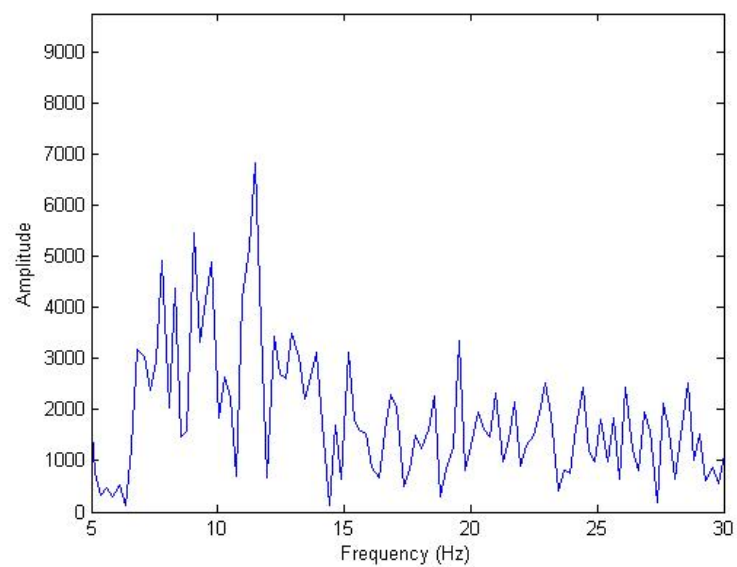


Figure 2.16: Recorded EEG spectrum of Oz Electrode for 7.5 Hz SSVEP stimulation

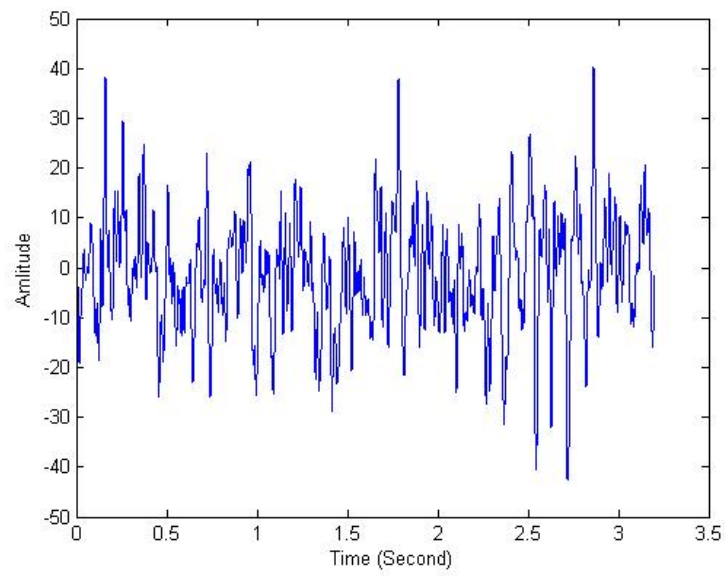


Figure 2.17: Recorded EEG waveform of Oz Electrode for 8.2 Hz SSVEP stimulation

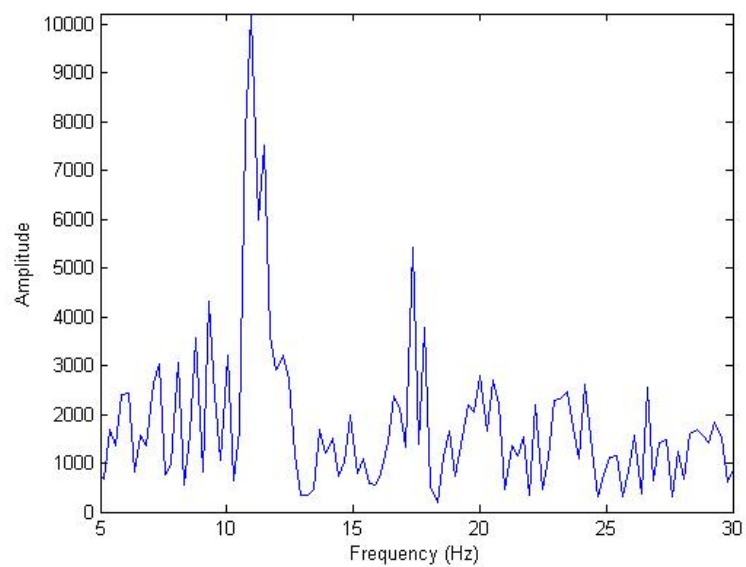


Figure 2.18: Recorded EEG spectrum of Oz Electrode for 8.2 Hz SSVEP stimulation

Chapter 3

Robotic Vehicle Control

To control a robotic vehicle, first a communication channel needs to be established first. The robot would decode the control signals received over the communication channel or link and turn or move accordingly [24–26]. Control signal generation is done by the matlab script. When the user interface loads, the matlab searches for the com terminal specified by the scripts. The robotic vehicle uses a hot-pluggable USB-to-TTL converter to connect to the computer. So if the robot is connected to the computer, only then the com port is present. If the matlab script finds the terminal specified, only then a matlab object is created for interacting and controlling the robotic vehicle. Else, it is not used. The scripts functions normally if the robotic vehicle is not present. Only that, no control signal is generated from the matlab for the purpose of robotic vehicle control [27–29].

3.1 Robotic Vehicle

The robot contains an USB-TTL converter based on PL2303 IC [30], an Arduino Nano, L293D driver for driving 2 BO Motors attached to wheels, a DC-DC Step Down buck regulator to regulate the voltage supplied to motor [31]. The voltage regulation helps to regulate the motor speed. The arduino pro mini is so programmed that it can receive commands through the UART connection at 9600 baud [32] and it interprets the command to control the motors. Upon receiving a certain command it changes the control signals to the motor driver ic. It is possible to use HC-05 or HC-06

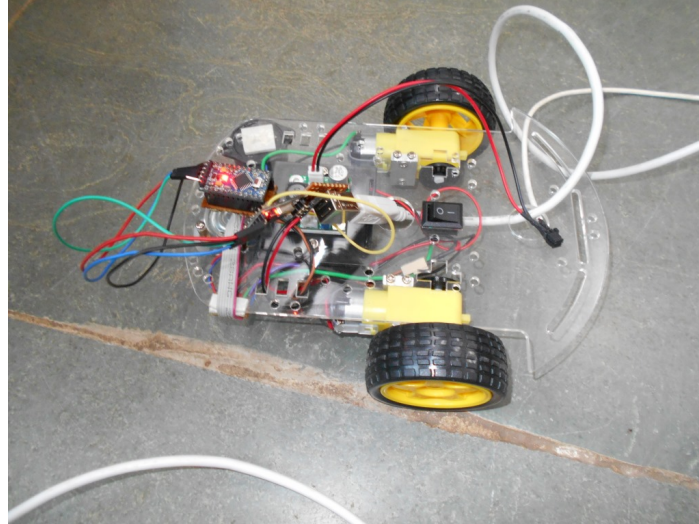


Figure 3.1: Robotic Vehicle

Bluetooth module to establish the wireless link via bluetooth and connect the vehicle to the computer/laptop [32, 33]. The arduino pro mini has inbuilt UART/USART module which is compatible with HC-06/HC-05 module [32, 34]. No modification or reprogramming is needed in the software. But if bluetooth module is used, a separate power module would be required as the PL2303 module supplies the 5V DC power to powerup the arduino pro mini and the control stage of L293 driver.

3.1.1 Power Requirements

The robotic vehicle needs proper distribution of power to all of its parts to function properly, low power supply would result in frequent reset, over voltage would cause damage to the components. Need of each part of the circuit is different. While the PL2303 USB-TTL converter IC has a low power requirement, it could be powered by USB. The Arduino pro mini also draws around 20 mA power. These two devices together can be powered via USB. But the motors connected draw 300 mA each while it has no load. And more if it is loaded. Also, while starting up, the motor draws a huge amount of current as a motor is an inductive load. The power supplied from the USB is around 1A and the voltage is 5V. So the motors cannot be powered via USB. So they need to be supplied with external power supply or battery. Also, supplying

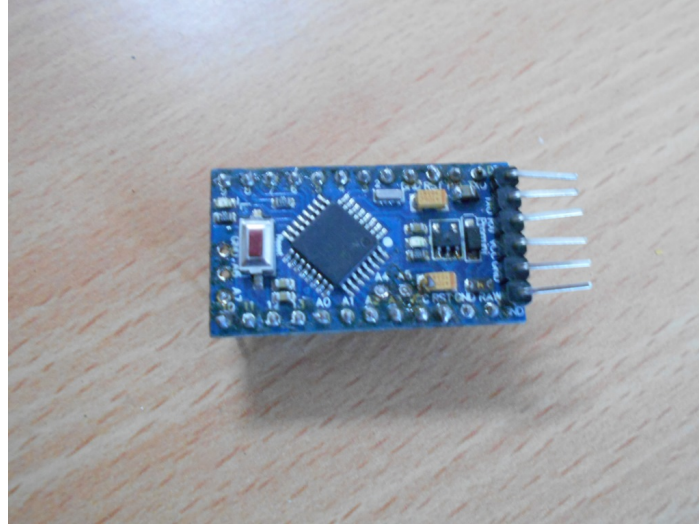


Figure 3.2: Controller (Arduino Pro Mini)

the motors from the USB poses risk to damage the USB port.

To handle the extra power required by the motors, L293D motor driver IC is used. This IC comes with two power supplies. One for the internal control circuitry. Another powersupply pin is used to connect to the supply for the motors. The output stage of L293D is made of Bipolar Junction Transistors. And if surge current flows through it, the internal power transistors might draw current from the control stage and resetting the transistor. To prevent this, electrolytic capacitors are used to supply extra power in case of power surge. Also, freewheeling diodes are connected in parallel to the motors in reverse bias condition to bypass the current generated when the motor is stopped. To suppress the surge peaks, electrolytic capacitors are used across the motor terminals.

For control signal generation, the detected SSVEP signal is converted to control signals using an interpretation-table supplied to the matlab object communicating with the robot. It eliminates the necessity to reprogram the robots when flickering frequencies are changed for experimenting with other frequencies.

For wheelchair control, mainly five options are required to be detected to go forward, go backward, turn left, turn right and to stop. The frequencies assigned are 6, 6.5, 7, 7.5 and 8.2 Hz respectively. The options are arranged in the UI as shown in the figure. The background of the uiwindow is kept black. And it starts in the fullscreen

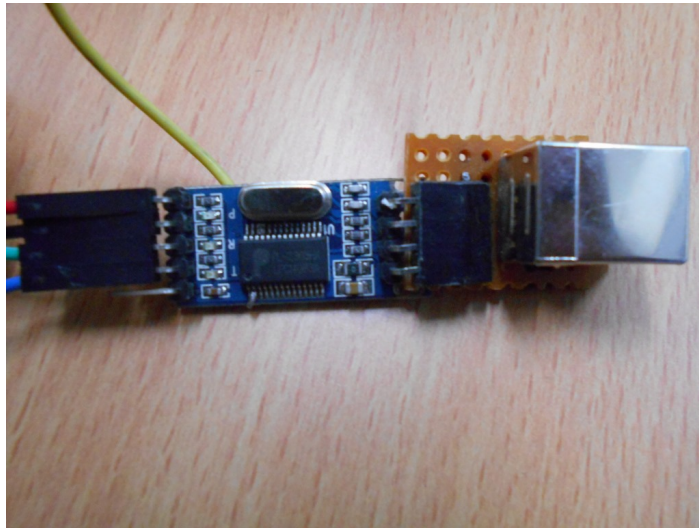


Figure 3.3: USB to TTL converter module

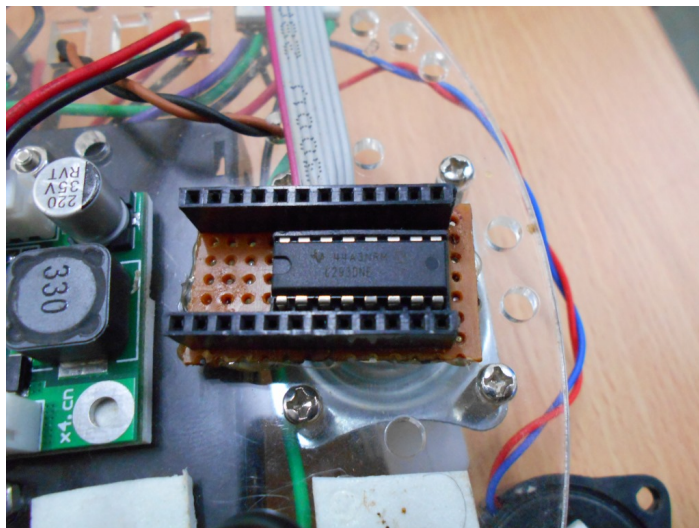


Figure 3.4: Motor Driver Unit

mode to stop other programs from interfering with the it. The Symbols are UTF-16 symbols supported by java. The symbols are colored dark gray, and the surrounding areas of each individual symbols are divided into white rectangles. To make the area surrounding the symbol flicker, the white rectangles are programmatically made to appear and disappear periodically.

3.2 Speed Control

The robotic vehicle need to maintain a moderate speed for operation. Too high acceleration is not suitable in this application, it would result accidents. The torque of a DC motor is directly proportional to the voltage supplied to the dc motor. Also, the speed of the motor can be controlled with a fixed voltage power source by pulse width modulating the control voltage to the motors. But the pulse width modulation control increases the complexity of the system, also, if the dc voltage source is varying, advance algorithm is needed to compensate for that voltage variation. However, that is out of the scope of this research. To maintain a modest speed, and to keep the control algorithm simple, a DC-DC buck Voltage Converter is used in the project. The buck converter is supplied with a 12V 1A SMPS and the buck converter is tuned to give 7.5V output to the L293D motor driver. The buck Converter employs LM2696 simple swither [35]. The LM2696 comes with a inbuilt voltage controlled pulse width modulator and has an external feedback system. The amount of voltage feedback can be regulated with an on board potentiometer provided in the module [35]. By varying the feedback voltage, the output voltage of the module can be controlled.

3.3 Operation

While starting, the user interface automatically calls up a matlab session in the background for data acquisition and analysis. To setup and run the experiment, the user interface executes command in the matlab and calls a script specified in the supplied json settings file. The script is called in four type of events, when the

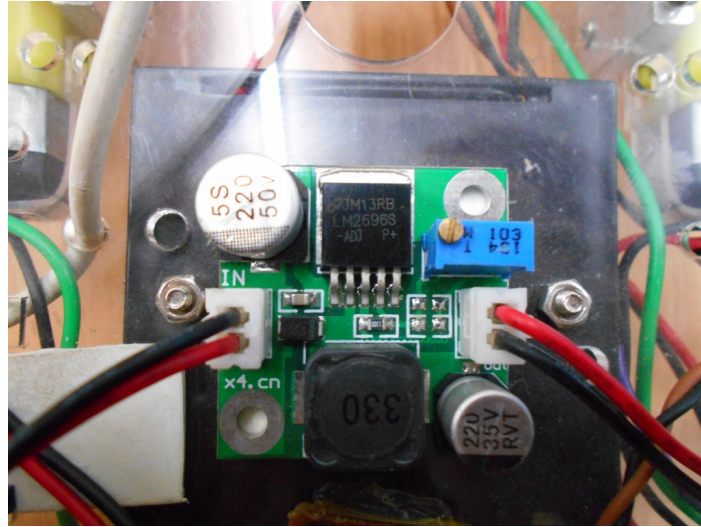


Figure 3.5: Picture of DC-DC Step Down Switching Voltage Regulator

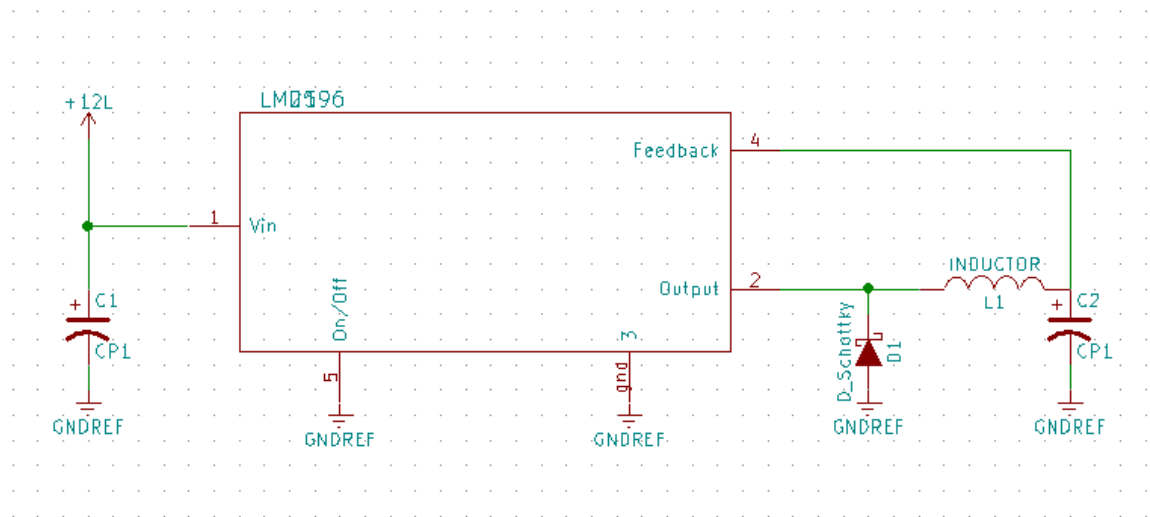


Figure 3.6: Reference Circuit Diagram of DC-DC Step Down Switching Voltage Regulator

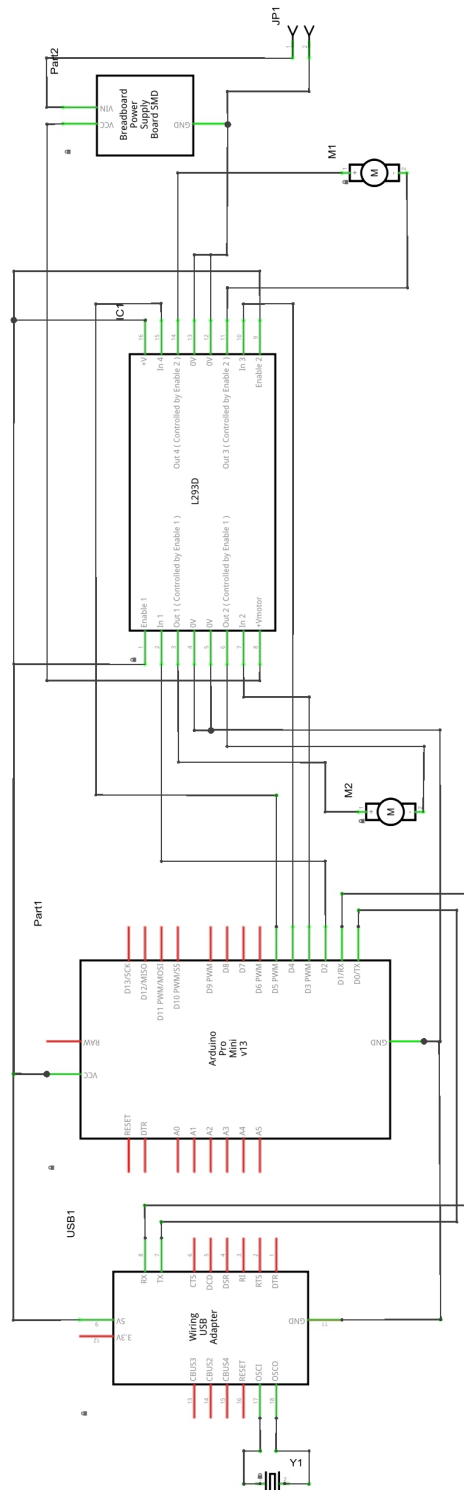


Figure 3.7: Circuit Diagram of Robotic Unit

json file is loaded, when the flickering is started by the start/stop button, each time when sampling is started, when sampling is stopped, and in a predetermined interval while sampling. The interval of calling up the matlab script is also determined by the settings file.

While starting up, the script calls up LabChart software to interface the data acquisition device. The script takes help of three other scripts to start the LabChart software, acquire data from the Powerlab 16/35 to the matlab, and stop data acquisition session.

The data is processed by matlab, it slices the acquired data and takes the collected samples for last 8 seconds for analysis. At the time of setting up experiment, an activex object is created for matlab to interact with labchart using ‘actxserver’ function call. Reference to the com object is stored in a matlab variable.

3.4 Methodology

The SSVEP analysis could be a single channel or multichannel. It depends on the availability of equipment and desired accuracy. Multichannel analysis has distinctive advantage of better detection accuracy. Any acquired EEG signal has a lot of interfering component from the other part of the brain. It is because every biopotential measurement is just a sum of all the biopotential generated in between two electrodes. The signals, that falls closer to the imaginary straight line joining them has strongest presense in those two electrodes. But ofcourse, part of them are still available in electrodes placed in the close viscinity of the two electrodes. This is know as ‘cocktail party problem’. It is possible to identify the presence of the interfering component in the EEG signal using multichannel SSVEP detection using Independent Component Analysis[36–38]. But multiple channel requires sophisticated hardware as the channel number is more. This includes multichannel biopotential measurement devices. Communication devices capable of increased data rate. Signal processing hardware capable of handling more computations.

Apart from interference, noise is also a big concern. In any biomedical

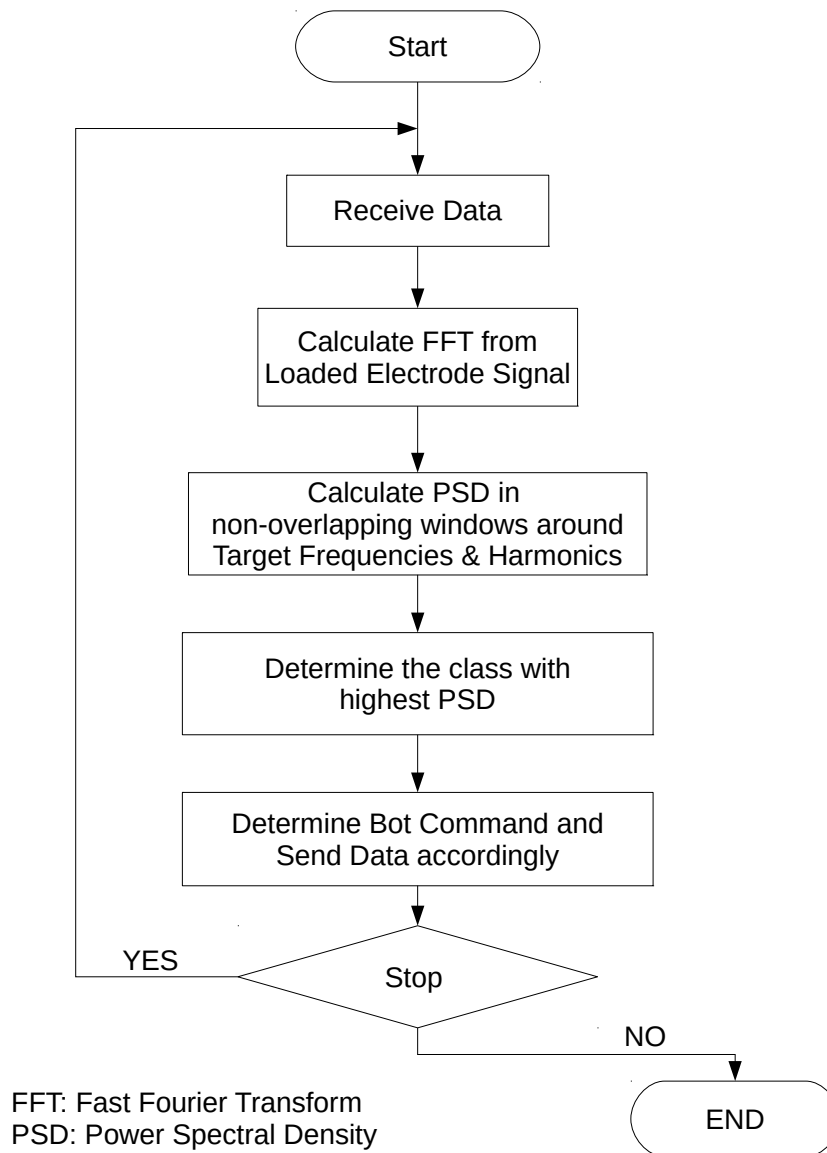


Figure 3.8: Control Flow Diagram

measurement, noise cannot be avoided, but using digital signal processing, the signal quality can be improved. However, simple filters are not sufficient in biomedical application. Especially in EEG signal processing. Many a times, the noise power cannot be removed using filters because it poses risk to reject the original signal generated from the human brain. Thus adaptive algorithms should be used for noise removal [39]. Later in this chapter, in section 3.4.2, we would see that the SSVEP signal contains multiple harmonics. thus we can also use comb filters besides adaptive algorithms to enhance the ssvep signals.

Single channel SSVEP detection records from one single channel Oz. And the other electrode at AFz is connected to the ground of the bio amplifier. For the reference potential, an electrode is connected to the Fz electrode. Single channel detection allows simplistic and minimal data acquisition to be used.

3.4.1 Preprocessing

One of the most important part of EEG signal processing is filtering. If the signal is not filtered by hardware, non adaptive filtering is done with the help of digital filters. Mostly band select filtering and notch filtering is done by the hardware. Another part of the preprocessing is downsampling [40, 41]. The SSVEP signal is strong for 4-60 Hz band. So 200 Hz and above frequency is a decent sampling frequency. If the EEG has a high sampling frequency (more than 500 Hz) we can reliably downsample the signal without affecting overall performance [42, 43]. More samples results increase in computation to take fourier transform of the sampled signal. All these three mentioned methods are part of eeg preprocessing. If not done by the data acquisition system, the algorithm needs modify to do these three preprocessing steps.

3.4.2 Mathematical Model

The SSVEP signal appears as a feature in the frequency spectrum. If the signal is strong enough and includes less noise, Canonical Correlation analysis could be performed. The signal sample needs to be first baseline restored in this type of analysis.

If, on the other hand, frequency based approach is used, then baseline restoration is optional. But if baseline restoration is used, then the low frequency, unnecessary components are removed. The frequency analysis is quite robust upto some levels of noise.

Suppose the flickering Frequency is f Hz, then if $y_i(t)$ is the signal obtained, then for electrode i we can model it as below:

$$y_i(t) = \sum_{K=1}^{N_h} a_{i,k} \sin(2\pi kft + \phi_{i,k}) + \sum_j b_{i,j} Z_j(t) + e_i(t) \quad (3.1)$$

From the equation above, we can see that it is a linear model, and it breaks down the signal into three components. The first term being the SSVEP itself. And we can see that it has a sinusoidal component and its harmonics. This is the component, we need to detect from the EEG signal. The sinusoids have electrode specific amplitude $a_{i,k}$ and phase $\phi_{i,k}$ respectively.

The second term is interference signals from the other part of the brain, EM interference and artifacts due to other physical movements, breathing artifacts etc. It is denoted as $z_j(t)$. Each sub component of interfering signals have different levels of interference. So they are multiplied with weight factors $b_{i,j}$.

Apart from the interference signals there is an electrode specific noise component $e_i(t)$. The noise component cannot be modelled. While performing the experiments, care should be taken to keep the SNR high. A low SNR would result in false detections and unexpected results.

The equation 3.1 can be expressed in vector form. For that we assume the sampling frequency to be F_s Hz, and sampling duration of N_t Seconds. The vector form of the equation is as below:

$$y_i = Xa_i + Zb_i + e_i \quad (3.2)$$

in the equation, $y_i = [Y_i(1), \dots, Y_i(N_t)]^T$ is a $N_t \times 1$ vector. e_i is a vector for noise with same dimension. The SSVEP Model Matrix X has a size of $N_t \times 2N_h$

$$X = [X_1 X_2 \dots X_{N_h}] \quad (3.3)$$

Each submatrix X_k contains a $\sin(2\pi kft)$ and $\cos(2\pi kft)$ pair in columns. The a_i vector corresponding to X_k is the amplitudes of X_k . It's length is $2N_h \times 1$.

From the first term, we can see that the SSVEP response has harmonics in the spectrum. As seen from experiments, the power is distributed in multiple frequencies and many a times, the harmonics contain more power than the fundamental frequency itself. Because of this, while classifying the received SSVEP signal, not only the fundamental frequency, but it's harmonics as well needs to be included by the classifier. To calculate the score for a class x classifying for frequency H , we calculate the score by the following equation.

$$C_x = \sum_{i=1}^N \sum_{iH-0.1}^{iH+0.1} |Y| \quad (3.4)$$

The class of the signal is then determined by $\max(C)$.

$$C_x \in C \quad (3.5)$$

The method includes extra harmonic components in calculation for classes whos fundamental frequency or it's harmonic frequency falls in the 9.5-12.5 Hz range. It results in improved accuracy for the classes. The reason for selecting more harmonics when thease frequencies are encountered is that the normal human brain activity generates α waves in this range. Extra harmonics reduces margin of error.

3.5 Results

Before the algorithm is used on the robotic vehicle to control it, it is tested on a standard database. Also, the algorithm is tested on the database prepared for offline analysis. This gave us a comparison of accuracy of our database compared to the standardd database. Also, algorithm is tested against standard database so that it's

accuracy is verified.

3.5.1 Standard Database

The standard database is obtained from [44]. It is used by Vilic et.al in his paper [1]. The database is recorded against 5 subjects. The ssvep excitation source was flickeing square targets on a LCD Screen, flickering at 6Hz, 6.5Hz, 7Hz, 7.5Hz, 8.2Hz. The Participant details are as follows.

Table 3.1: Details of participants in the multitarget standard database

Subject	Gender	Age
1	Male	32
2	Female	27
3	Male	27
4	Female	27
5	Male	26

The proposed algorithm is tested against standard database, and its performance is compared to the the standard database first. The first harmonics of 6Hz is at 12Hz. So due to normal brain activity, the power of 12 Hz could result in higher score in 6Hz class. So to reduce margin of error, third harmonics is included in the calculation. The result shows improvement for 6Hz Frequency class compared to the 8.2 Hz class. The accuracy of 8.2 Hx class remains unchanged. It is shown as below.

Table 3.2: Correct Detection Per User using Author's [1] method on standard database

Subject	6 Hz Accuracy (%)	8.2 Hz Accuracy	% Overall Accuracy
Subject 1	100	75	87
Subject 2	100	100	100
Subject 3	87.5	37.5	62.5
Subject 4	75	87.5	81.25
Subject 5	100	100	100

3.5.2 Developed Database

The proposed algorithm is by performance is equivalent to the standard database. The recorded database has four subject in trial, all male. The output result shows less

Table 3.3: Correct Detection Per User using modified method on standard database

Subject	6 Hz Accuracy (%)	8.2 Hz Accuracy	% Overall Accuracy
Subject 1	100	75	87
Subject 2	100	100	100
Subject 3	100	37.5	68.75
Subject 4	87.5	87.5	87.5
Subject 5	87.5	100	93.75

accuracy for recorded database. The participation details and the measured accuracy for generated database is as shown below.

Table 3.4: Details of participants in the multitarget standard database

Subject	Gender	Age
1	Male	25
2	Male	24
3	Male	24
5	Male	27

Table 3.5: Correct Detection Per User using modified method on generated database

Subject	6 Hz Accuracy (%)	8.2 Hz Accuracy	% Overall Accuracy
Subject 1	12.5	87.5	50
Subject 2	87.5	100	93.75
Subject 3	100	0	50
Subject 4	100	62.5	81.25

3.6 Discussion

When the data acquisition session starts, the the information about how many channels are being sampled, and sampling frequency of each of them are recorded. The data is transferred in short intervals, multiple samples at a time. At the time of setting up the experiment, a matlab script is registered using 'registerevent' function call. Each time the data arrives, the function is called to process the data. The data is arranged inside this function, the sample for last few second is copied and passed to the analysis script for analysis and control signal generation. The method is tested on the standard database obtained from [44].

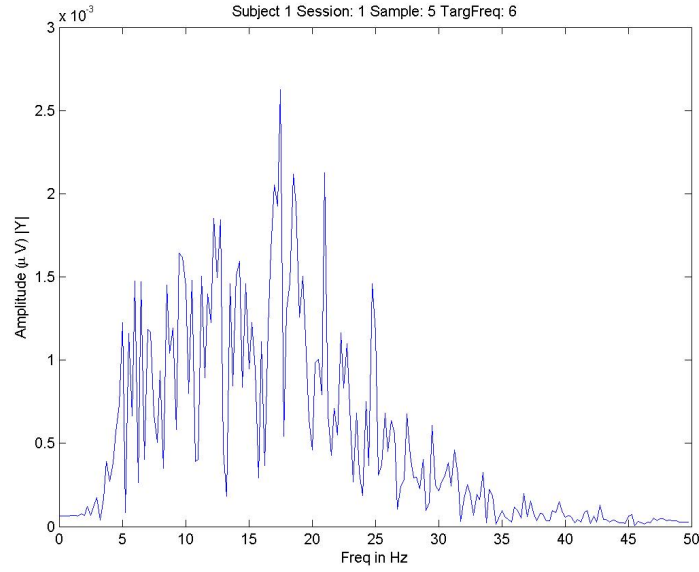


Figure 3.9: EEG Spectrum of Oz Channel for 6 Hz Excitation Source

Here are the spectrums and the classification results from the standard database. Figure 3.9 is the spectrum of ssvep signal obtained for subject 1 in session 1. The sample is recorded for the 6Hz target. Thus in the spectrum we can see there is a peak on 6Hz, 12Hz and 18Hz. Figure 3.10 is the bar graph of the score of the classes claculated from the spectrum. Similarly, for 6.5Hz, 7 Hz, 7.5Hz and 8.2Hz SSVEP stimulation, the spectrums ae Figure 3.11, Figure 3.13, Figure 3.15 and Figure 3.17 respectively. And the respective classification scores are shown in Figure 3.12, Figure 3.14, Figure 3.16 and Figure 3.18.

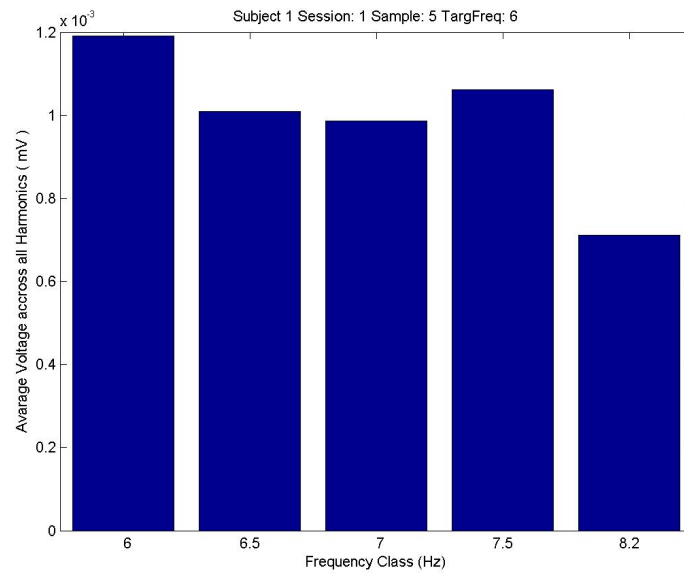


Figure 3.10: Classifier Scores for Each Class with dominant 6 Hz Class

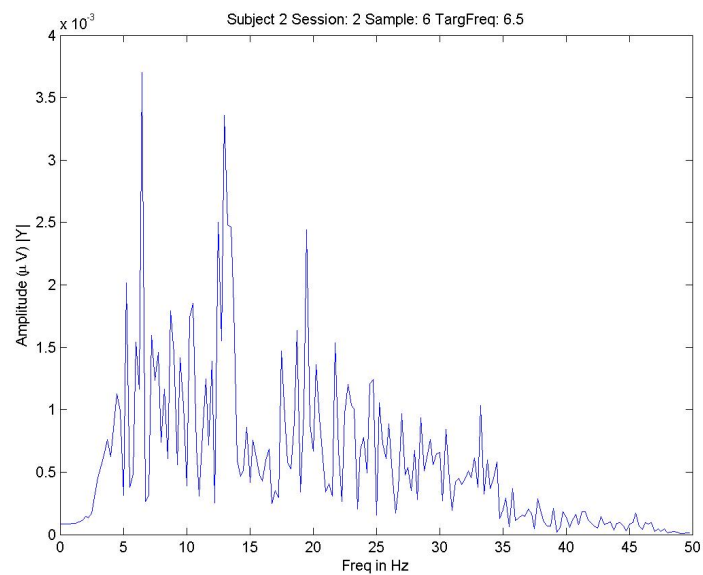


Figure 3.11: EEG Spectrum of Oz Channel for 6.5 Hz Excitation Source

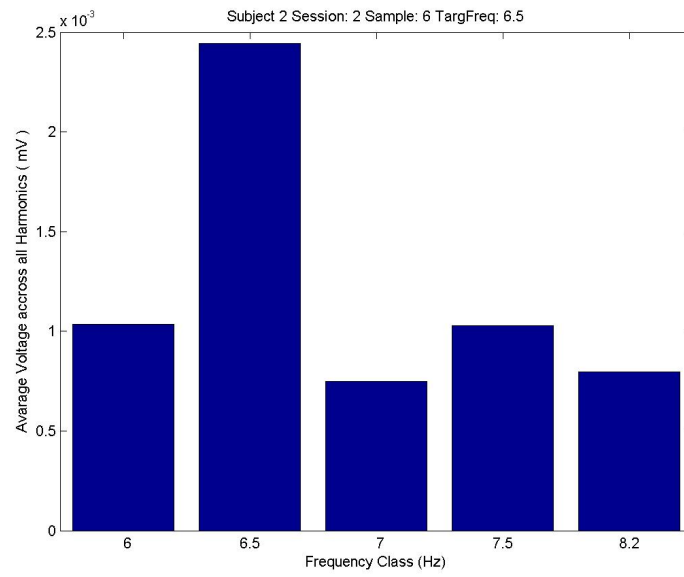


Figure 3.12: Classifier Scores for Each Class with dominant 6.5 Hz Class

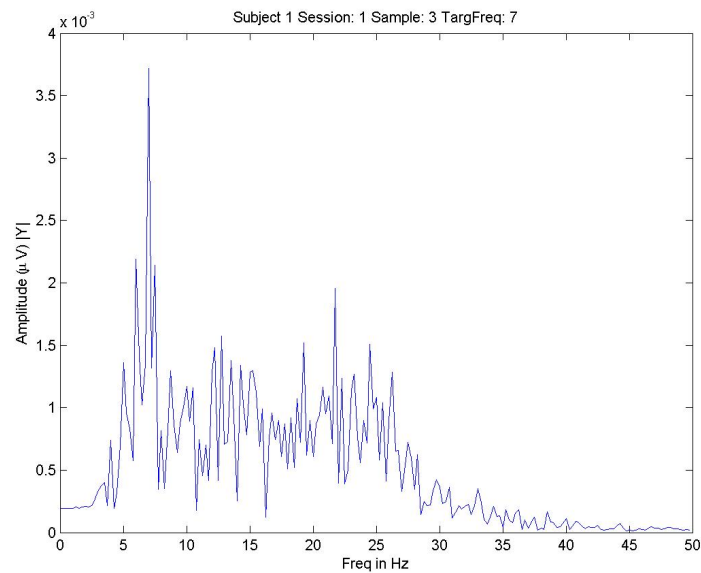


Figure 3.13: EEG Spectrum of Oz Channel for 7 Hz Excitation Source

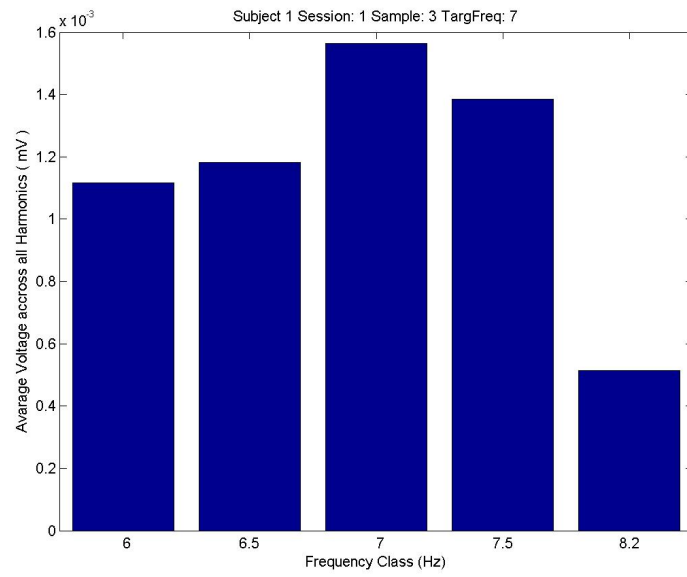


Figure 3.14: Classifier Scores for Each Class with dominant 7 Hz Class

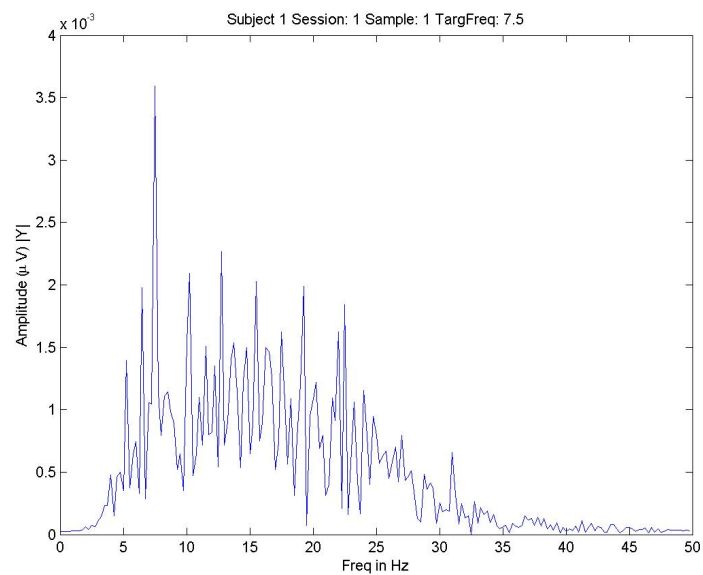


Figure 3.15: EEG Spectrum of Oz Channel for 7.5 Hz Excitation Source

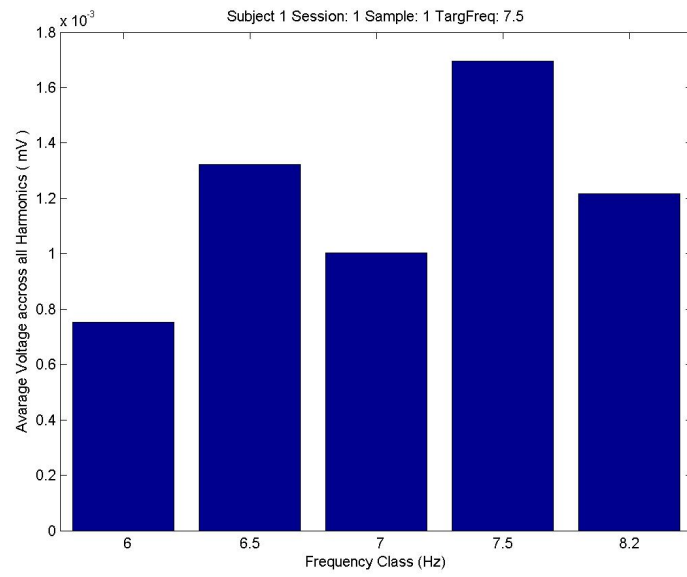


Figure 3.16: Classifier Scores for Each Class with dominant 7.5 Hz Class

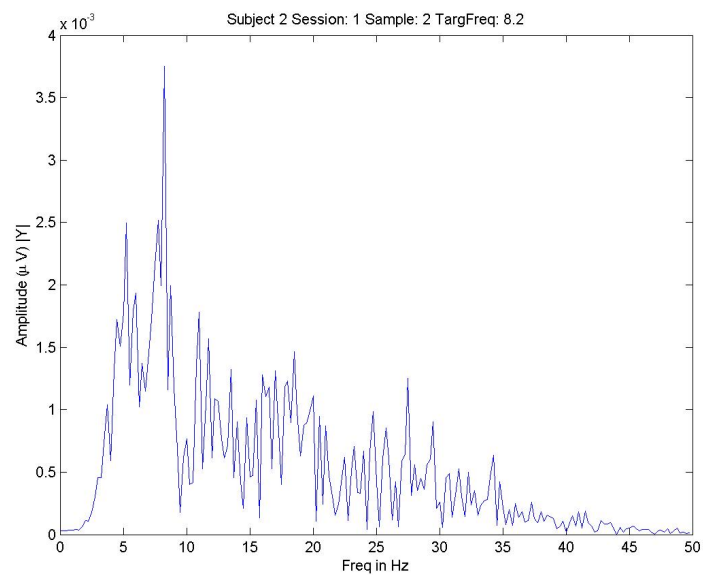


Figure 3.17: EEG Spectrum of Oz Channel for 8.2 Hz Excitation Source

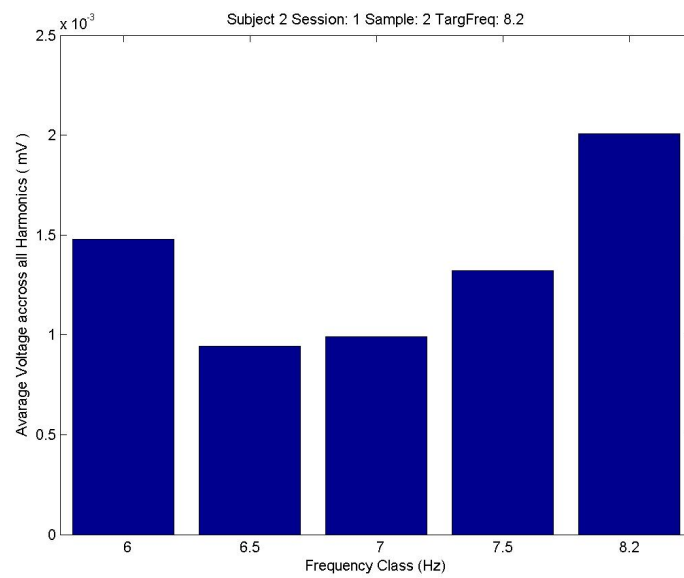


Figure 3.18: Classifier Scores for Each Class with dominant 8.2 Hz Class

Chapter 4

Conclusion and Future Work

4.1 Conclusion

- In this work, one application of brain computer interface has been demonstrated. The brain computer interface is implemented using an Electroencephalogram Machine, and a computer.
- A robotic platform has also been built and controlled by the brain computer interface. A similar system could be used in an electric wheelchair with modifications to the wheelchair to accept and interpret the commands into actions.
- The work shows a possible applications for persons with spinal cord injuries to provide them some mean of mobility without human assistance. However, the reliability of this system needs to be improved before bringing it to application.

4.2 Future work

- As discussed in chapter 1, the SSVEP response is not uniform through out the spectrum. So, while classifying the SSVEP signal, the score of each class should be scaled using adaptive algorithms, such as MCTW [45], for better accuracy. Adaptive algorithms have been reported to increase accuracy[22, 46–48] .
- The Electrode lead wires acts as an antenna for the external electromagnetic

waves[39]. If the system accuracy improves beyond 90%, by implementing previous suggestion, then a system incorporating eeg frontend and digital signal processor could be used to reduce the size the overall system and reduce connection length to further improve the system accuracy.

- As discussed in chapter 1, disabled persons needs assistance for even communicating. The user interface, as discussed in chapter 2.1 is designed to accomodate more applications of brain computer interface. It would be really helpful if we can extend the functionality of this system as a substitute of the keyboard[49].
- When the BCI system is being used in the consumer's environment, many of unwanted interference would appear in the signal. Ambient conditions are more noisy than the laboratory environment. So, noise removal should be included in the application [50].

References

- [1] A. Vilic, T. W. Kjaer, C. E. Thomsen, S. Puthusserypady, and H. B. D. Sorensen, “Dtu bci speller: an ssvep-based spelling system with dictionary support,” in *Engineering in Medicine and Biology Society (EMBC), 2013 35th Annual International Conference of the IEEE*. IEEE, 2013, pp. 2212–2215.
- [2] G. Pfurtscheller, D. Flotzinger, and J. Kalcher, “Brain-computer interface a new communication device for handicapped persons,” *Journal of Microcomputer Applications*, vol. 16, no. 3, pp. 293–299, 1993.
- [3] D. Regan, “Steady-state evoked potentials,” *JOSA*, vol. 67, no. 11, pp. 1475–1489, 1977.
- [4] S. P. Kelly, E. C. Lalor, R. B. Reilly, and J. J. Foxe, “Visual spatial attention tracking using high-density ssvep data for independent brain-computer communication,” *Neural Systems and Rehabilitation Engineering, IEEE Transactions on*, vol. 13, no. 2, pp. 172–178, 2005.
- [5] H. Bakardjian and A. Cichocki, “Classification of fast imagined motion responses for a human-computer interface,” in *Proc of Jap Soc for Med and Biol Engin Conf*, vol. 462, 2003.
- [6] S. P. Koch, J. Steinbrink, A. Villringer, and H. Obrig, “Synchronization between background activity and visually evoked potential is not mirrored by focal hyperoxygenation: implications for the interpretation of vascular brain imaging,” *The Journal of neuroscience*, vol. 26, no. 18, pp. 4940–4948, 2006.
- [7] C. E. Davila, R. Srebro, and I. A. Ghaleb, “Optimal detection of visual evoked potentials,” *IEEE Transactions on Biomedical Engineering*, vol. 45, no. 6, pp. 800–803, 1998.
- [8] H. Bakardjian, T. Tanaka, and A. Cichocki, “Optimization of ssvep brain responses with application to eight-command brain-computer interface,” *Neuroscience letters*, vol. 469, no. 1, pp. 34–38, 2010.
- [9] S. Tobimatsu, H. Tomoda, and M. Kato, “Normal variability of the amplitude and phase

- of steady-state veps,” *Electroencephalography and Clinical Neurophysiology/Evoked Potentials Section*, vol. 100, no. 3, pp. 171–176, 1996.
- [10] G. R. Burkitt, R. B. Silberstein, P. J. Cadusch, and A. W. Wood, “Steady-state visual evoked potentials and travelling waves,” *Clinical Neurophysiology*, vol. 111, no. 2, pp. 246–258, 2000.
- [11] J.-J. Vidal, “Toward direct brain-computer communication,” *Annual review of Biophysics and Bioengineering*, vol. 2, no. 1, pp. 157–180, 1973.
- [12] C. S. Herrmann, “Human eeg responses to 1–100 hz flicker: resonance phenomena in visual cortex and their potential correlation to cognitive phenomena,” *Experimental brain research*, vol. 137, no. 3-4, pp. 346–353, 2001.
- [13] O. Friman, I. Volosyak, and A. Gräser, “Multiple channel detection of steady-state visual evoked potentials for brain-computer interfaces,” *IEEE Transactions on Biomedical Engineering*, vol. 54, no. 4, pp. 742–750, 2007.
- [14] M. T. Akhtar, C. J. James, and W. Mitsuhashi, “Modifying the spatially-constrained ica for efficient removal of artifacts from eeg data,” in *2010 4th International Conference on Bioinformatics and Biomedical Engineering (iCBBE)*. IEEE, 2010, pp. 1–4.
- [15] L. Astolfi, F. Cincotti, D. Mattia, F. Babiloni, M. G. Marciani, F. D. V. Fallani, M. Mattiocco, F. Miwakeichi, Y. Yamaguchi, P. Martinez *et al.*, “Removal of ocular artifacts for high resolution eeg studies: a simulation study,” in *Engineering in Medicine and Biology Society, 2006. EMBS’06. 28th Annual International Conference of the IEEE*. IEEE, 2006, pp. 976–979.
- [16] T.-P. Jung, S. Makeig, M. Westerfield, J. Townsend, E. Courchesne, and T. J. Sejnowski, “Removal of eye activity artifacts from visual event-related potentials in normal and clinical subjects,” *Clinical Neurophysiology*, vol. 111, no. 10, pp. 1745–1758, 2000.
- [17] W. De Clercq, A. Vergult, B. Vanrumste, J. Van Hees, A. Palmi, W. Van Paesschen, and S. Van Huffel, “A new muscle artifact removal technique to improve the interpretation of the ictal scalp electroencephalogram,” in *Engineering in Medicine and Biology Society, 2005. IEEE-EMBS 2005. 27th Annual International Conference of the*. IEEE, 2006, pp. 944–947.
- [18] A. Cichocki and S.-i. Amari, *Adaptive blind signal and image processing: learning algorithms and applications*. John Wiley & Sons, 2002, vol. 1.
- [19] H. Ghandeharion and H. Ahmadi-Noubari, “Detection and removal of ocular artifacts using independent component analysis and wavelets,” in *4th International IEEE/EMBS Conference on Neural Engineering, 2009. NER’09*. IEEE, 2009, pp. 653–656.

-
- [20] P. S. Kumar, R. Arumuganathan, K. Sivakumar, C. Vimal *et al.*, “An adaptive method to remove ocular artifacts from eeg signals using wavelet transform,” *J. Appl. Sci. Res.*, vol. 5, no. 7, pp. 711–745, 2009.
- [21] J. Mejia-García, J. Martínez-de Juan, J. Saiz, J. García-Casado, and J. Ponce, “Adaptive cancellation of the ecg interference in external electroenterogram,” in *Engineering in Medicine and Biology Society, 2003. Proceedings of the 25th Annual International Conference of the IEEE*, vol. 3. IEEE, 2003, pp. 2639–2642.
- [22] F. Beverina, G. Palmas, S. Silvoni, F. Piccione, and S. Giove, “User adaptive bcis: Ssvep and p300 based interfaces,” *PsychNology Journal*, vol. 1, no. 4, pp. 331–354, 2003.
- [23] W. Philips, “Adaptive noise removal from biomedical signals using warped polynomials,” *IEEE Transactions on Biomedical Engineering*, vol. 43, no. 5, pp. 480–492, 1996.
- [24] A. Mohebbi, S. K. D. Engelholm, S. Puthusserypady, T. W. Kjaer, C. E. Thomsen, and H. B. D. Sorensen, “A brain computer interface for robust wheelchair control application based on pseudorandom code modulated visual evoked potential,” in *Engineering in Medicine and Biology Society (EMBC), 2015 37th Annual International Conference of the IEEE*, Aug 2015, pp. 602–605.
- [25] A. Mohebbi, S. K. Engelholm, S. Puthusserypady, T. W. Kjaer, C. E. Thomsen, and H. B. Sorensen, “A brain computer interface for robust wheelchair control application based on pseudorandom code modulated visual evoked potential,” in *Engineering in Medicine and Biology Society (EMBC), 2015 37th Annual International Conference of the IEEE*. IEEE, 2015, pp. 602–605.
- [26] Y. Li, J. Pan, F. Wang, and Z. Yu, “A hybrid bci system combining p300 and ssvep and its application to wheelchair control,” *IEEE Transactions on Biomedical Engineering*, vol. 60, no. 11, pp. 3156–3166, 2013.
- [27] P. F. Diez, S. M. T. Müller, V. A. Mut, E. Laciari, E. Avila, T. F. Bastos-Filho, and M. Sarcinelli-Filho, “Commanding a robotic wheelchair with a high-frequency steady-state visual evoked potential based brain–computer interface,” *Medical engineering & physics*, vol. 35, no. 8, pp. 1155–1164, 2013.
- [28] G. Bin, X. Gao, Y. Wang, Y. Li, B. Hong, and S. Gao, “A high-speed bci based on code modulation vep,” *Journal of neural engineering*, vol. 8, no. 2, 2011.

-
- [29] M. Cheng, X. Gao, S. Gao, and D. Xu, "Design and implementation of a brain-computer interface with high transfer rates," *IEEE Transactions on Biomedical Engineering*, vol. 49, no. 10, pp. 1181–1186, 2002.
- [30] (2016, Jun.) Pl2303hx usb to serial bridge controller. [Online]. Available: http://www.prolific.com.tw/UserFiles/files/ds_pl2303HxD_v1_4_4.pdf
- [31] (2016, Jun.) L293x quadruple half-h drivers. [Online]. Available: <http://www.ti.com/lit/ds/symlink/l293.pdf>
- [32] (2016, Jun.) Arduino pro mini. [Online]. Available: <https://www.arduino.cc/en/Main/arduinoBoardProMini>
- [33] (2016, Jun.) Hc-06 bluetooth smart modules. [Online]. Available: http://www.csr.com/sites/default/files/microchip_bttmp_data_sheet_feb_15.pdf
- [34] (2016, Jun.) Atmega328p atmel 8-bit microcontroller. [Online]. Available: http://www.atmel.com/images/atmel-8271-8-bit-avr-microcontroller-atmega48a-48pa-88a-88pa-168a-168pa-328-328p_datasheet_complete.pdf
- [35] (2016, Jun.) Lm2596 simple switcher. [Online]. Available: <http://www.ti.com/lit/ds/symlink/lm2596.pdf>
- [36] A. Hyvärinen, J. Karhunen, and E. Oja, *Independent component analysis*. John Wiley & Sons, 2004, vol. 46.
- [37] A. Hyvärinen and E. Oja, "Independent component analysis: algorithms and applications," *Neural networks*, vol. 13, no. 4, pp. 411–430, 2000.
- [38] A. Hyvärinen, "Fast and robust fixed-point algorithms for independent component analysis," *Neural Networks, IEEE Transactions on*, vol. 10, no. 3, pp. 626–634, 1999.
- [39] M. Ferdjallah and R. E. Barr, "Adaptive digital notch filter design on the unit circle for the removal of powerline noise from biomedical signals," *IEEE Transactions on Biomedical Engineering*, vol. 41, no. 6, pp. 529–536, 1994.
- [40] R. Aler, I. M. Galván, and J. M. Valls, "Evolving spatial and frequency selection filters for brain-computer interfaces," in *Evolutionary Computation (CEC), 2010 IEEE Congress on*. IEEE, 2010, pp. 1–7.
- [41] G. Gómez-Herrero, W. De Clercq, H. Anwar, O. Kara, K. Egiazarian, S. Van Huffel, and W. Van Paesschen, "Automatic removal of ocular artifacts in the eeg without an eeg reference

- channel,” in *Signal Processing Symposium, 2006. NORSIG 2006. Proceedings of the 7th Nordic*. IEEE, 2006, pp. 130–133.
- [42] T. S. Mukesh, V. Jaganathan, and M. R. Reddy, “A novel multiple frequency stimulation method for steady state vep based brain computer interfaces,” *Physiological Measurement*, vol. 27, no. 1, p. 61, 2005.
- [43] J. R. Wolpaw, N. Birbaumer, D. J. McFarland, G. Pfurtscheller, and T. M. Vaughan, “Brain–computer interfaces for communication and control,” *Clinical neurophysiology*, vol. 113, no. 6, pp. 767–791, 2002.
- [44] (2016, Jun.) Adnan vilic. [Online]. Available: <https://www.setzner.com>
- [45] Z. İscan and Z. Dokur, “A novel steady-state visually evoked potential-based brain–computer interface design: character plotter,” *Biomedical Signal Processing and Control*, vol. 10, pp. 145–152, 2014.
- [46] A. Turnip, K.-S. Hong, and S. Yoon, “Adaptive nonlinear principle component analysis based multilayer neural network for p300 detection,” in *System Integration (SII), 2011 IEEE/SICE International Symposium on*. IEEE, 2011, pp. 96–99.
- [47] E. Yin, Z. Zhou, J. Jiang, Y. Yu, and D. Hu, “A dynamically optimized ssvep brain–computer interface (bci) speller,” *IEEE Transactions on Biomedical Engineering*, vol. 62, no. 6, pp. 1447–1456, 2015.
- [48] H. Cecotti and A. Gräser, “Convolutional neural networks for p300 detection with application to brain–computer interfaces,” *Pattern Analysis and Machine Intelligence, IEEE Transactions on*, vol. 33, no. 3, pp. 433–445, 2011.
- [49] M. S. Treder, N. M. Schmidt, and B. Blankertz, “Gaze-independent brain–computer interfaces based on covert attention and feature attention,” *Journal of neural engineering*, vol. 8, no. 6, p. 066003, 2011.
- [50] M. A. G. Correa and E. L. Leber, *Noise removal from EEG signals in polisomnographic records applying adaptive filters in cascade*. INTECH Open Access Publisher, 2011.